PERMEABILITY OF INTESTINAL CAPILLARIES

Pathway followed by Dextrans and Glycogens

NICOLAE SIMIONESCU, MAIA SIMIONESCU, and GEORGE E. PALADE

From The Rockefeller University, New York 10021. Doctors N. and M. Simionescu's permanent address is the Institute of Endocrinology, Bucharest, Romania.

ABSTRACT

The pathway followed by macromolecules across the wall of visceral capillaries has been studied by using a set of tracers of graded sizes, ranging in diameter from 100 A (ferritin) to 300 A (glycogen). Polysaccharide particles, i.e. dextran 75 (mol wt ~75,000; diam ~125 A), dextran 250 (mol wt 250,000; diam ~225 A), shellfish glycogen (diam ~200 A) and rabbit liver glycogen (diam ~300 A), are well tolerated by Wistar-Furth rats and give no vascular reactions ascribable to histamine release. Good definition and high contrast of the tracer particles were obtained in a one-step fixation—in block staining of the tissues by a mixture containing aldehydes, OsO_4 and lead citrate in phosphate or arsenate buffer, pH 7.4, followed by lead staining of sections. The glycogens and dextrans used move out of the plasma through the fenestrae and channels of the endothelium relatively fast (3–7 min) and create in the pericapillary spaces transient (2–5 min) concentration gradients centered on the fenestrated sectors of the capillary walls. The tracers also gained access to the plasmalemmal vesicles, first on the blood front and subsequently on the tissue front of the endothelium. The particles are temporarily retained by the basement membrane. No probe moved through the intercellular junctions. It is concluded that, in visceral capillaries, the fenestrae, channels, and plasmalemmal vesicles, viewed as related parts in a system of dynamic structures, are the structural equivalent of the large pore system.

INTRODUCTION

The pathway followed by large molecules (diam. ≥100 A) across the wall of visceral capillaries has been studied so far only in the intestinal mucosa of the mouse, using ferritin (diam. ~100 A) as a tracer (1). An extension of the inquiry to larger probes is highly desirable for the following reasons: (*a*) It is of interest to find out whether molecules of larger dimensions than ferritin follow a common or a different pathway. (*b*) In the first alternative, the pathway can be identified as the structural equivalent of the large pore system. According to the pore theory of capillary permeability (2–5), the large pores should be permeable to molecules or particles up to ~500 A diameter. (*c*) In intestinal capillaries, the diameter of the smallest molecules that move exclusively through large pores is still in question: it has been estimated as ≥220 A by Mayerson et al. (3), but there are reasons to believe (cf. 1, 2) that it is ≥90 A.

We have recently shown that glycogens and dextrans can be used as tracer molecules in electron microscope studies of capillary permeability (6) and now we present results obtained with five tracers of graded size ranging in diameter from ~100 A (ferritin) to ~300 A (glycogen) in

work done on the capillaries of the intestinal mucosa of the rat. All these tracers behave like ferritin in the previous experiments: they leave the plasma–definitely–through a fraction of the total fenestral population of the endothelium, and–probably–through plasmalemmal vesicles. Accordingly, these elements are identified as the structural equivalent of the large pore system in the endothelium of visceral capillaries.

MATERIALS AND METHODS

Materials

TRACERS

The following tracers were used:

(a) DEXTRAN 75 (D75)[1-2]: mol wt 75,000; mol diam ~125 A, obtained as a 6% w/v solution in 0.9% NaCl from Abbott Laboratories, North Chicago, Ill.

(b) DEXTRAN 250 (D250)[1-2]: mol wt ~250-000 A; mol diam ~225 A, obtained as Dextran Grade A Clinical, from Schwarz/Mann, Orangeburg, N. Y.

(c) SHELLFISH GLYCOGEN (SG)[1-2]: mol diam ~200 A.

(d) RABBIT LIVER GLYCOGEN (RLG)[1-2]: mol diam ~300 A, both obtained from Schwarz/Mann.

The preparation of tracer solutions, the tests for vascular leakage, and the procedures to determine particle size and dispersion (by negative and positive staining) are described in (6). After injection in the blood stream, the latter parameters were checked by negative staining of plasma samples.

(e) FERRITIN: prepared as described in (1), was used in a few experiments to ascertain if it follows the same pathways across the endothelium as in the intestinal capillaries of the mouse.

[1] Conventional abbreviations adopted for the tracers used.

[2] Dextrans of larger molecular weight, e.g.: DT 500 (mol wt ~500,000), DT 2000 (mol wt ~2,000-000), both from Pharmacia Fine Chemicals Inc., Piscataway, N. J. and from Sigma Chemical Co., St. Louis, Mo. and dextran, mol wt 5–40,000,000 from Nutritional Biochemicals Corporation, Cleveland, Ohio, proved to be less convenient on account of size heterogeneity and tendency to form aggregates. Particles heterogeneity also affects other glycogens tested, e.g. oyster glycogen, diameter ~100–350 A (from Calbiochem., Los Angeles, Calif.) and beef liver glycogen (from Nutritional Biochemicals Corporation), which is a mixture of α and β particles.

ANIMALS

The experiments were performed on 234 male, young adult (100–135 g) rats of the Wistar-Furth strain (Microbiological Associates, Inc., Bethesda, Md.), known to be genetically resistant to histamine release by dextrans (7) and glycogens (6). The use of male rats obviates possible variations in circulation during the sexual cycle and the choice of young animals avoids the increase in blood pressure and the modifications of the ground substance in the lamina propria of small intestine which occur in aging rodents (8). For a few days before the experiments, all animals were kept under standardized conditions of housing and feeding which included a final 24 hr fasting.

Control animals were used to check the morphology of the capillaries in the absence of circulating tracers and to assess possible changes induced by 24 hr starvation.

Methods

EXPERIMENTAL PROCEDURE

ANESTHESIA: Ether was preferred since it induces negligible changes in the blood volume and pressure (9, 10). For postinjection intervals longer than 15 min the animals were allowed to wake up and anesthetized again at the end of the interval.

TRACER INJECTION: 1 ml/100 g body weight of tracer solutions was slowly (20–30 sec) injected into the saphenous vein. Since the average heart rate of an anesthetized rat is ~425 per min (11), and since ~140–210 cardiac cycles occur during the injection, the circulation time of the tracers was counted from the beginning of the injection.

The injected volume was adjusted to 10% of the estimated total blood volume (12). For the amounts used, and applying the van't Hoff's equation for dilute solutions ($\pi = cRT$), the contribution of the injected tracers to the colloid osmotic pressure of the plasma was less than 1%.

We assume that with the volumes and concentrations injected, there are small and transient changes in plasma volume and plasma protein concentration (cf. 13, 14).

FIXATION *IN SITU*-BLOOD FLOW ARREST: At chosen intervals (Table I) a ~3 cm long jejunal loop was isolated *in situ* by ligatures at both ends, one of them being placed around a Yale-hypodermic needle No. 26G ½ inch previously introduced into the intestinal lumen (Fig. 1 a). The fixative was injected into the lumen of the loop through this needle and at the same time poured over its peritoneal surface and dripped on the vasa recta and corresponding branches of the mesenteric vessels. The blood vessels of the loop were not ligated, to avoid stressing effects and to fix the tissue while circulation

TABLE I

*Number of Rats Used for Each Time Point in Tracer Experiments**

Tracers	TIME POINTS‡															Total number of animals (234)
	1.5	2	2.5	3	4	5	6	8	11	16	30	1	2	4	24	
	min	*min*	*min*	*min*	*min*	*min*	*min*	*min*	*min*	*min*	*min*	*hr*	*hr*	*hr*	*hr*	
Rabbit liver glycogen	2	2	4	4	8	2	6	7	4	1	2	2	2	3	4	53
Shellfish glycogen	2	4	4	4	9	6	7	3	3	1	2	2	2	2	4	55
Dextran 250		4		10	5	6	3	3	3	2		2	2		2	42
Dextran 75	2	10	2	9	6	3	5	7	7	7	2	2	2		2	66
Ferritin				2	2	2		2								8
Control animals (non-injected)																10

* For each animal, five to eight samples of small intestine (villi) were examined by electron microscopy.
‡ Counted from the beginning of the injection (and including an additional minute as average estimated lag for the arrest of blood flow by fixation *in situ*).

was still going on. Fixation continued for 10 min *in situ* insured the regular retention of plasma and tracers in the vascular lumina.

TIME REQUIRED FOR THE ARREST OF BLOOD FLOW BY THE FIXATIVE: To determine the time required for particle transport across the capillary wall, data concerning the lag between the beginning of fixation and the arrest of local blood circulation are needed. This lag was timed in two different types of preparations: (*a*) the loop and its mesentery, and (*b*) the villi. For (*a*), a loop was exteriorized under anesthesia from the abdominal cavity; it was isolated as described, placed in a transparent lucite dish, and covered with a thin layer of Ringer's solution at 36–38° C. The fixative was injected into the lumen and applied simultaneously to the outer surface of the loop and to the mesentery while the circulation in (*i*) mesentery vessels, (*ii*) vasa recta, and (*iii*) intramural vessels (see Fig. 1 a) was observed under a light microscope at 100 to 400 ×. For (*b*) the loop was split open along the antimesentery margin and the circulation in the villi observed at ~500 × while fixative was layered over the mucosa. The vascular network can be reasonably well visualized in villi, oriented perpendicularly to the optical axis of the microscope.

The lag was found to be of 40–60 sec for the vessels of the villi and of 80–130 sec for those visible under the mucosa and in the mesentery. Lag variations induced by changes in fixative temperature (from 0° to 36°C) were small or negligible for the circulation of the villi.

In a few experiments, specimens were taken for further processing from the area of early circulation arrest. In the majority of the experiments specimens were collected from the middle of loops fixed *in situ* without systematically checking the blood flow. Since in the majority of our experiments we used as fixative a cooled (~4° C) mixture of aldehydes, OsO_4 and lead citrate (see: One-Step Fixation–Staining in Block), the estimated lag is of ~1 min. In the observations which follow, all time points were corrected for this value.

TISSUE PROCESSING: After 10 min fixation *in situ*, the middle third of the intestinal loop was excised and strips (0.5 mm × 1 mm) of the already hardened intestinal wall were cut from the antimesenteric region. For further fixation, the strips were immersed in the same solution.

The following *fixatives* and *fixation procedures* were used:

Two Step Fixation (*a*) *Fixation* in 5% glutaraldehyde + 3% formaldehyde (undiluted or diluted 1:1 with the buffer) (15, modified procedure), in 0.1 M phosphate buffer, pH 7.4, at 0° C, for 2 hr; no washing; postfixation in 2% OsO_4 in 0.1 M phosphate buffer, pH 7.4, at 0° C for 2 hr. (*b*) Differs from (*a*) at the *postfixation* step which was carried out in a mixture of equal volumes of 2% OsO_4 in 0.1 M phosphate buffer pH 7.4 and of a saturated solution of lead citrate in the same buffer.

One-Step Fixation–Staining in Block For this procedure, the following stock solutions were used: A = 3% formaldehyde + 5% glutaraldehyde; B = 2% OsO_4; C = saturated solution of lead citrate.

All solutions were prepared in either 0.1 M phosphate or 0.1 M arsenate buffer, pH 7.4.

Despite its low solubility in these buffers and, con-

sequently, its low concentration (~2–3 mg%), the presence of lead throughout fixation results in intense staining of the polysaccharide particles and increases the contrast of cellular structures as can be seen on unstained sections (Figs. 2 a, 2 b). Solution A should be freshly prepared (15); the others can be kept at 4° C for weeks.

FIXING SOLUTION: The fixative solution is prepared by mixing in a cold graduated test tube 3 volumes of solution A, 2 volumes of solution B, and 1 volume of solution C. Throughout the procedure, the vials, the stock solutions, and the mixture should be kept in an ice bath. At higher temperatures the solution turns slightly brown, but no precipitates form. The fresh and cold mixture is clear, colorless, and has a pH of 7.2–7.4. At the end of the fixation period (1–2 hr), the solution may turn slightly brown.

Of the three fixation procedures used, the one-step method afforded the best results: it insures intensive staining of polysaccharide particles which are well visible even before section staining and concomitantly provides good preservation and adequate contrast of endothelial structures.

TISSUE STAINING IN BLOCK: Staining in block in either (*a*) unbuffered solution of Mg–uranyl acetate or uranyl acetate (16), or (*b*) uranyl acetate–oxalic acid mixtures buffered with 0.1 M *s*-collidine, pH 7.2 (18) proved of limited use because of partial glycogen extraction, reduction of differential contrast between the tracers and plasma proteins, and production of fine precipitates within the tissue.

DEHYDRATION AND EMBEDDING: Without washing, all tissues were rapidly (35 min) dehydrated in cold (4° C) graded ethanols and embedded in Epon (19), either in capsules or in flat molds (20). The latter technique makes possible a suitable orientation of the villi for transverse sectioning (Fig. 1 b). Stained thick sections (0.5–1.0 μ) were used to select a capillary-rich villus (Fig. 1 c) around which the final trimming of the block was centered.

Sections of ~600 A thickness, showing silver-to-grey interference colors, were cut with Dupont diamond knives on a MT2 Porter-Blum ultramicrotome. Usually the sectioning was done at three different levels of a villus: subapical, middle, and basal, and the appearance of the capillaries at the different levels compared.

For each animal, five to eight villi were studied

General Abbreviations

bm, basement membrane
c, blood capillary
cf, collagen fibrils
ch, channel
e, endothelium
ep, epithelium
f, fenestrae
fb, fibroblast
ge, endogenous glycogen
j, junction
l, lumen
m, macrophage
p, pericyte
pcs, pericapillary space
rbc, red blood cell
t, tracer particles
v, plasmalemmal vesicles

All figures show blood capillaries and associated tissues in the villi of rat jejunal mucosa. All specimens illustrated in the paper were prepared by one-step fixation and staining in block in the mixture containing aldehydes, osmium tetroxide, and lead citrate in arsenate buffer (Figs. 2 b, 14, 15 b, 15 c, 19, 20, 21) or in phosphate buffer (the other figures) (see Methods). All sections were stained in lead citrate except for those presented in Fig. 1 (stained by methylene blue), and Figs. 2 a and 2 b (unstained).

FIGURE 1 a Photograph of the usual experimental set up. An exteriorized intestinal loop had been isolated by two ligatures (*lg*), the one on the left tied over the needle (*n*) through which the fixative was injected into the intestinal lumen. The region from which specimens were collected is marked *t*. The sites at which the vasculature was surveyed to determine the time at which circulation stopped after the beginning of fixation are marked 1, 2, 3. *mb*, mesenteric branches; *vr*, vasa recta; *imb*, intramural branches.

FIGURE 1 b Flat embedding of a small strip of intestinal wall (*iw*) (jejunum) showing the position of the villi (*v*). × 10.

FIGURE 1 c Photomicrograph of a transverse section through a jejunal villus. The epithelium is marked *ep* and its brush border *bb*. In the core of the villus (lamina propria), nine profiles of blood capillaries (c_1–c_9) can be recognized, all of them located immediately under the epithelium. The profile of the central lymphatic is marked *cl*. The cellular elements of the lamina belong to a variety of types which can be more reliably identified in Fig. 3. × 1000.

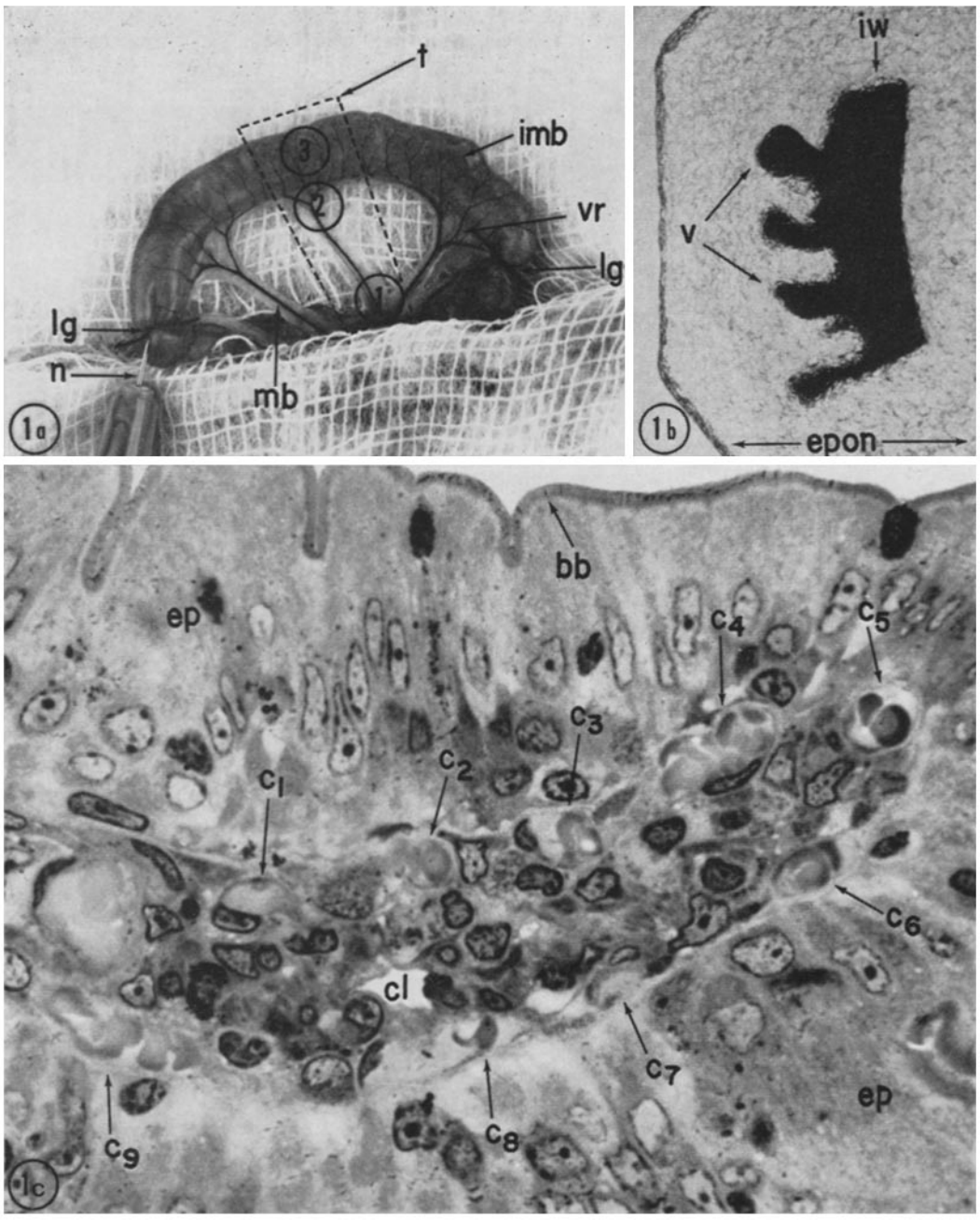
t
imb
3
2
1
vr
lg
lg
n
mb
1a
iw
v
1b
epon
bb
ep
c4
c5
c3
c2
c1
c6
cl
c7
ep
c9
c8
1c

and for each villus enough sections were examined to cover from 1 to 10% of its volume.

The sections were stained with lead citrate (21), or doubly stained with magnesium uranyl acetate and lead hydroxide or lead citrate (22). The examinations were made with a Siemens Elmiskop I or a Hitachi H-11C electron microscope operated at 80 kw and 75 kw, respectively, and provided with a 200 μ condenser II aperture, and a 50 μ objective aperture. The instruments were calibrated with a cross lined carbon grating replica having 2160 lines/mm.

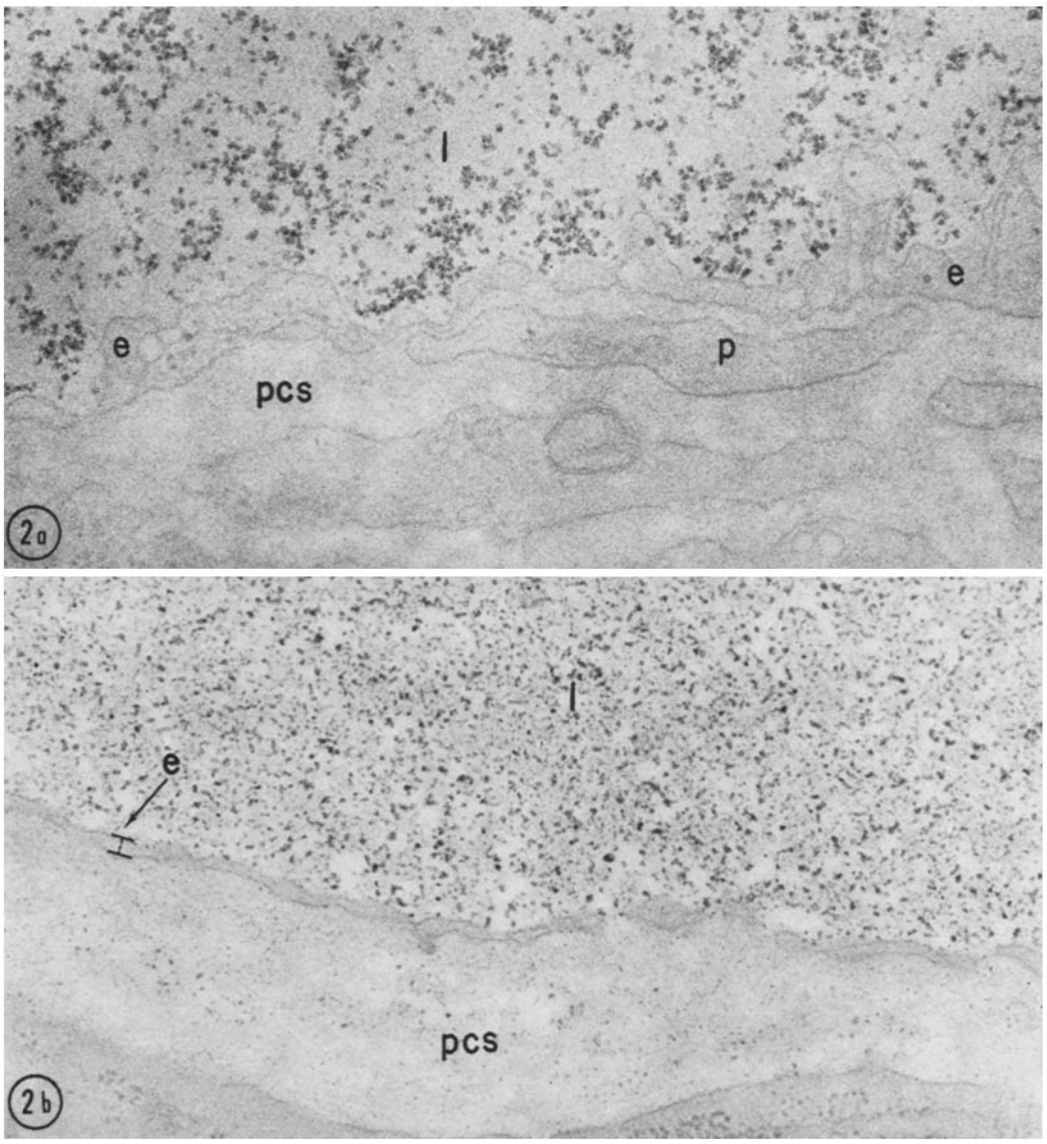

FIGURES 2 a–2 b Unstained sections of tissue specimens fixed and stained in block in one step with a mixture of aldehydes-OsO_4 and Pb citrate (see Methods). The micrographs show that block staining by lead imparts enough density to particulate glycogen (Fig. 2 a) and dextran (Fig. 2 b) to make the tracers visible without further staining of the sections. Fig. 2 a, rabbit liver glycogen, 2 min after i.v. injection. Fig. 2 b, dextran 75, 5 min after i.v. injection. Note the lack of tracer particles in the pericapillary spaces in Fig. 2 a and their presence in Fig. 2 b. Note also the difference in average size between the dextran particles in the lumen and those in the pericapillary spaces in Fig. 2 b. × 50,000.

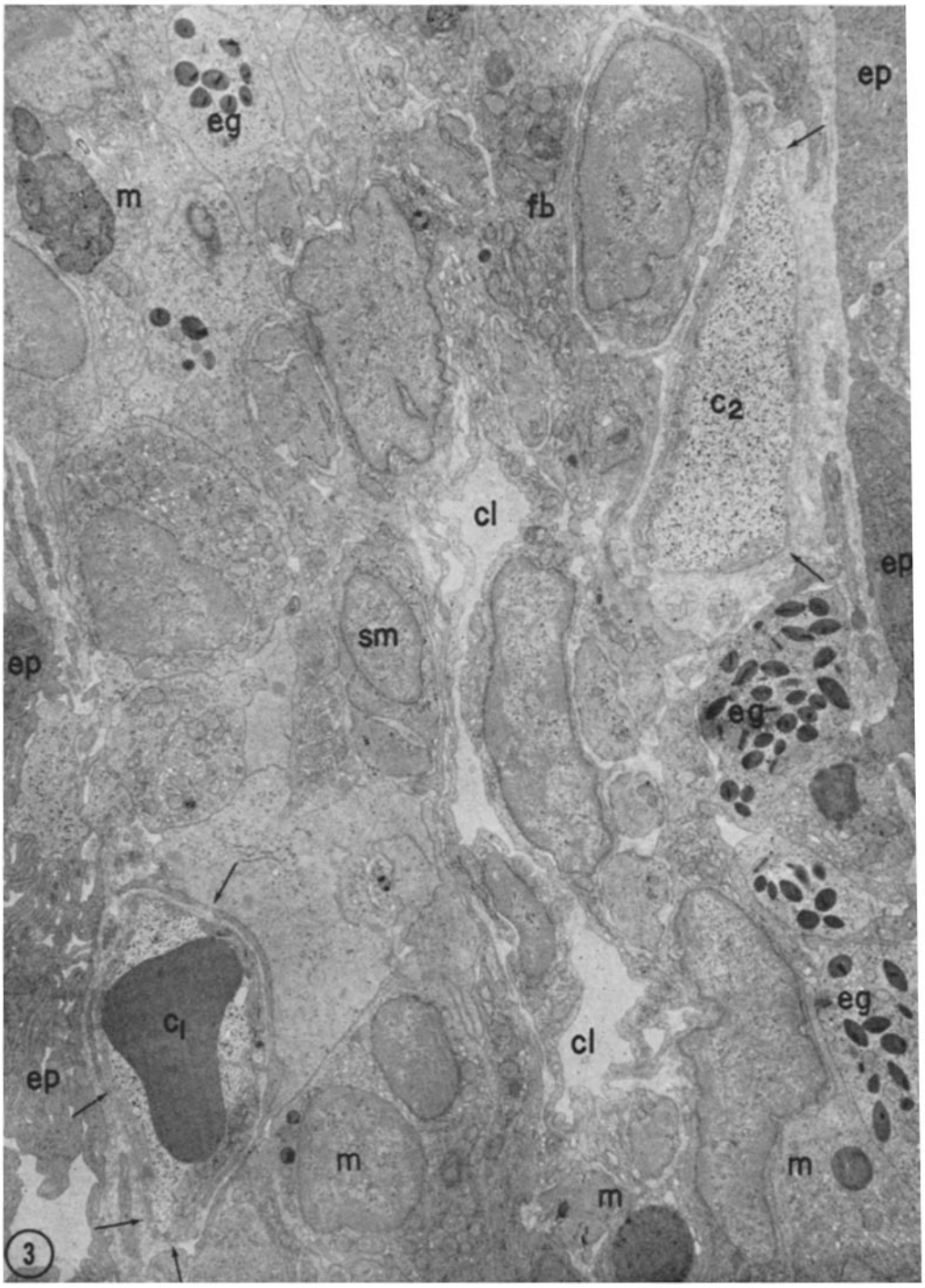

FIGURE 3 Low power electron micrograph of the core of a jejunal villus. The epithelium (*ep*) can be seen along the left and right margins. Two blood capillaries (c_1, c_2) located in the lamina propria face the adjacent epithelium mostly with the attenuated, fenestrated part (arrows) of their endothelial tunic. The central lacteal is sectioned obliquely at *cl*. Macrophages (*m*), eosinophil granulocytes (*eg*), smooth muscle cells (*sm*), fibroblasts (*fb*), and other cell types populate this region of the lamina propria. × 7800.

QUANTITATIVE MEASUREMENTS: Area measurements for estimating the concentration of glycogen particles were made on electron micrographs with a Keuffel and Esser planimeter and a calibrated 7 × magnifying glass.

RESULTS

Our observations concern primarily the blood capillaries of jejunal villi of the rat intestinal mucosa. Their structure is similar to that of the

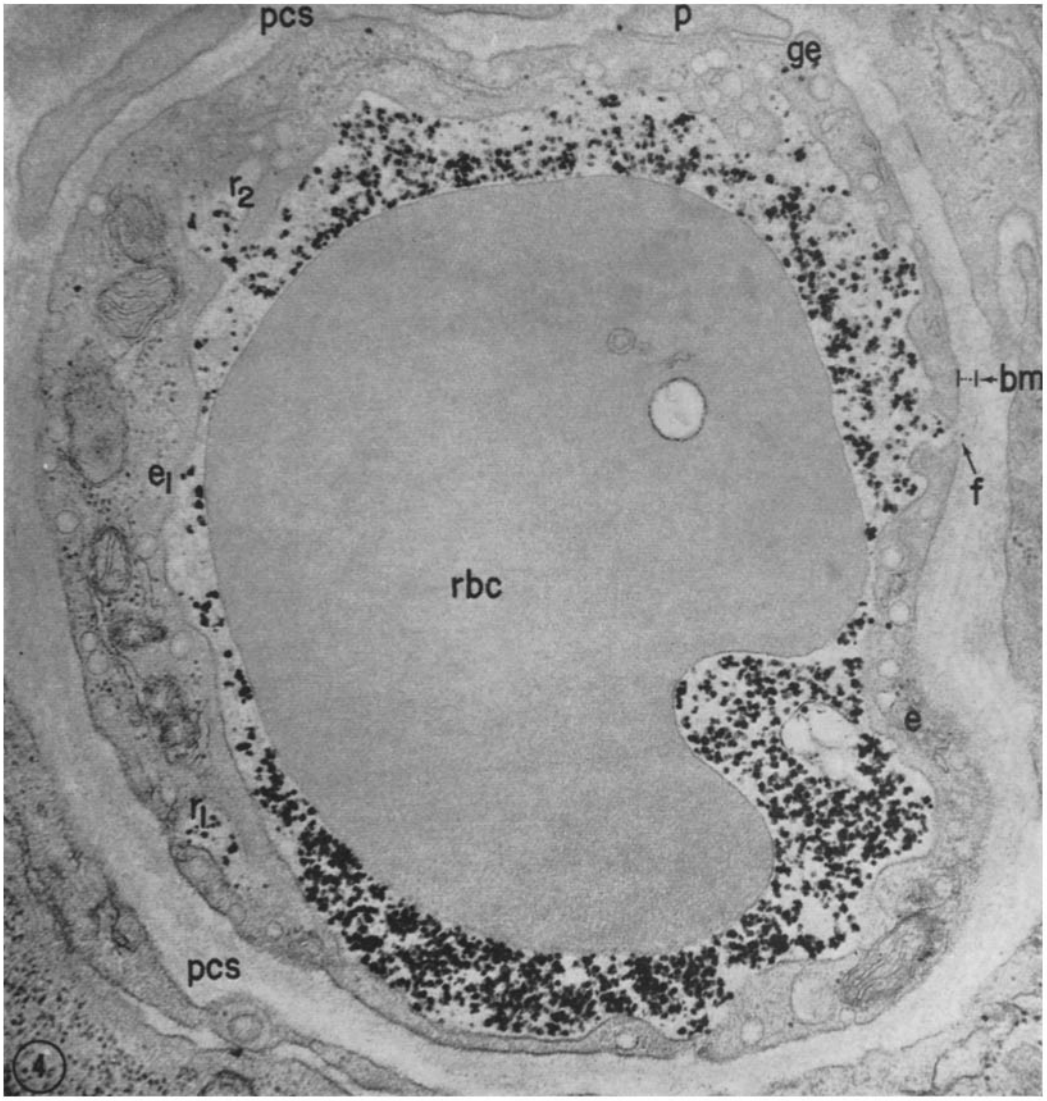

FIGURE 4 Blood capillary 2 min after an i.v. injection of rabbit liver glycogen. The tracer particles are nearly evenly distributed in the plasma, have access to two recesses (r_1, r_2), and have penetrated a shallow infundibulum leading to the fenestra marked *f*. A glycogen particle has traversed the fenestra and appears embedded in the basement membrane (*bm*). At this time point, the pericapillary spaces are free of tracer. Part of the lumen is occupied by an erythrocyte (*rbc*). The thicker part of the endothelial cell (e_1) contains mitochondria, elements of rough endoplasmic reticulum, and free polysomes. Endogenous glycogen particles are marked *ge*. × 40,000.

FIGURE 5 Blood capillary 4 min after an i.v. injection of shellfish glycogen. Tracer particles appear in high concentration and nearly even distribution in the lumen (*l*), in small clusters between the endothelium and the basement membrane (*bm*) (long arrows) and as individual particles in the pericapillary space (*t*). Some of the endothelial fenestrae have been penetrated by the tracer (short arrows); others appear to be impermeable (arrowheads). A cell junction appears at *j*. Note the difference in the concentration of the tracer between areas of the pericapillary spaces facing the fenestrated (lower half) and nonfenestrated (upper half) of the endothelium. × 28,000.

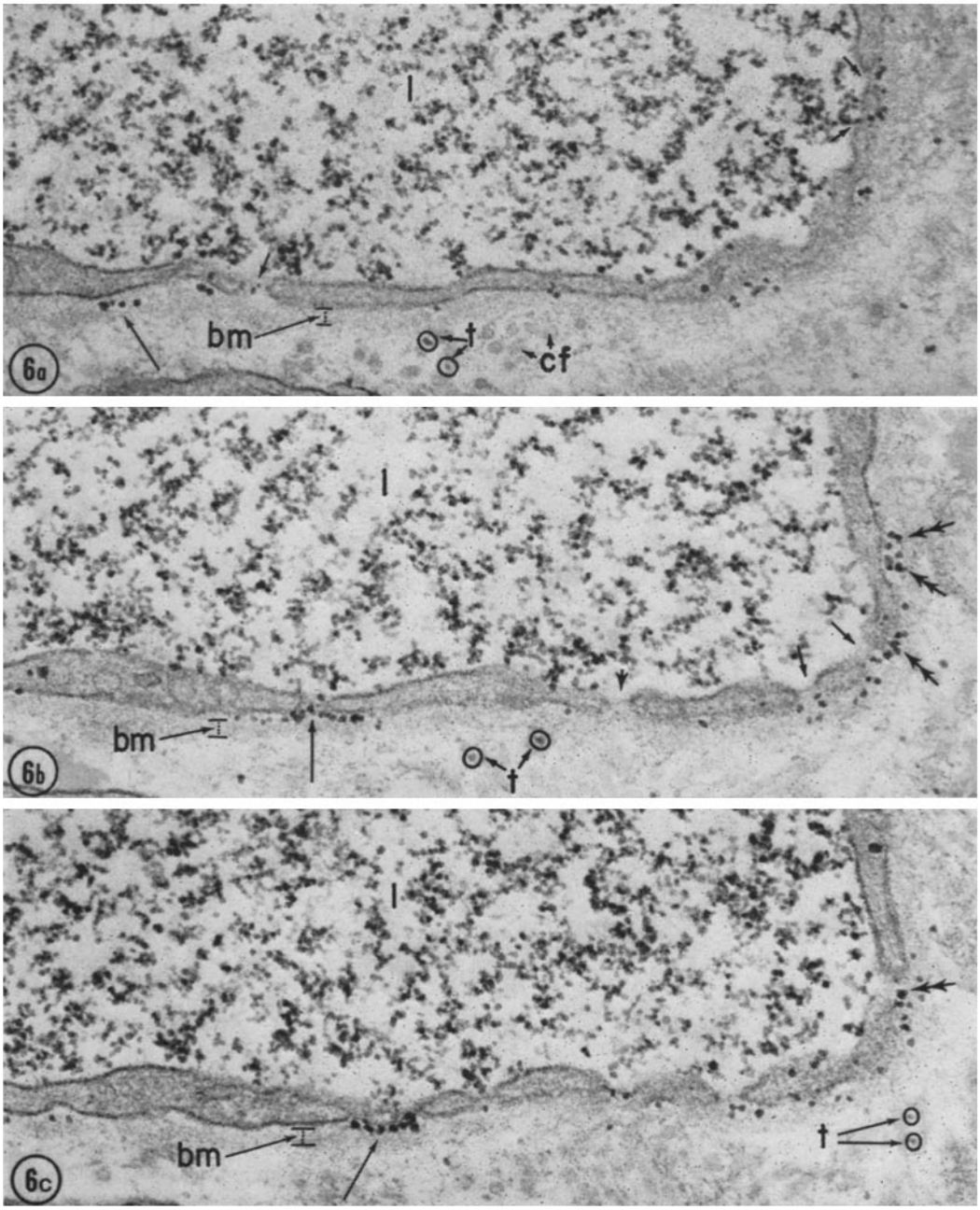

FIGURE 6 Three serial, nonconsecutive sections through a sector of the blood capillary in Fig. 5. They illustrate the presence of permeable (short arrows) and nonpermeable fenestrae (arrowhead) within the same region of the endothelium, the presence of small "clouds" of escaping particles opposite permeable fenestrae (double arrows), and the accumulation of particles, often spread in a single plane (long arrows) between the endothelium and the basement membrane (*bm*). Tracer particles in the pericapillary spaces are marked *t* Fig 6 b is an enlargement of part of Fig. 5. × 62,000.

corresponding vessels of the mouse (1): like the latter they have an endothelium with extensive fenestrated regions, preferentially oriented towards the base of the intestinal epithelium (Fig. 3). The structure of the vessels does not show detectable differences at the three levels examined within the villi, i.e. apex, middle, and base; nor does it change in response to our experimental variables, i.e. feeding or fasting, and presence or absence of tracers in the circulating plasma and the interstitial fluid. We preferentially used animals having fasted for 18–24 hr since they have few or no chylomicrons in the interstitia of the lamina propria and in the lacteals.

Polysaccharide Tracers

Early Events (Up to ⌣ 10 Min)

Our observations show that there are variations in the degree of filling of capillaries and in the rate of movement of tracers from the plasma to the interstitial fluid. Since these variations appear to be more pronounced along the length of the villus than at the same transversal level within the villus, we decided to concentrate our observations on the middle segment.

PLASMA: From the beginning of the observations, the tracers appear in high concentration and usually uniform distribution in the plasma: there is no, or negligible, aggregation of glycogen molecules, and although the dextrans frequently show some degree of aggregation, the clusters formed are few and small enough not to interfere with the observations. There is evident uptake of polysaccharide particles by platelets (Fig. 13 a) and leukocytes in circulation and variable adsorption of particles to the surface of erythrocytes. There is no adsorption of glycogen, but there is detectable adsorption of dextrans to the luminal surface of the endothelium.

As already noted (6), the glycogen molecules retain their size and shape in the circulating plasma (Figs. 2 a, 4), whereas the dextran particles are frequently distorted (Figs. 2 b, 14, 19), presumably on account of stresses developed during fixation. Glycogen and dextran particles recovered from the plasma 10 min after injection and examined by negative staining show no detectable differences in size, by reference to dimensions measured in solution before injection; hence there is no evidence of enzymic degradation, aggregation, or complex formation with plasma proteins within the short intervals investigated. The aggregation of dextran particles seen in many tissue specimens (cf. Figs. 14 and 19) most probably occurs during fixation.

ENDOTHELIUM: From the earliest time points, the tracers gain access to the shallow infundibula leading to the fenestrae and channels of the endothelium (Figs. 4, 14). SG and D75 particles were detected on the abluminal side of the fenestrae at 3–4 min (Figs. 5, 6, 14); for RLG and D250 molecules the corresponding figures are 5–7 min. Initial passage occurs through a fraction of the whole fenestral population (Table II), which varies from 20 to 70% from one capillary to another (Figs. 5, 8, 20). The permeable fenestrae appear to be distributed at random (rather than clustered) over the fenestrated part of the endothelium: in sections, permeable and nonpermeable fenestrae often occur within the same row (Figs. 5, 6, 8, 20). Most of the permeable fenestrae are marked by only one or two tracer particles, but quite often clusters of as many as 20 particles are found in the subendothelial space opposite a permeable fenestra (Table II[3] and Figs. 5, 6 b, 6 c). The state of the diaphragm of such fenestrae is difficult to assess: quite often there is suggestive evidence for the presence (Figs. 6–9, 15 b, 21 a, 21 b), rather than for the complete absence, of such a structure. Hence, permeant fenestrae are not necessarily diaphragm-free. The situation is the same for diaphragmed channels (Figs. 8, 9, 15 a) in which tracer particles appear in all positions expected for a tracer in transit, from adluminal to the proximal diaphragm, to abluminal to the distal one. For D250, there is suggestive evidence that the particles (or aggregates thereof) unravel as they move through endothelial fenestrae (Figs. 20, 21 a, 21 b).

From the earliest time points, tracer particles are also found in the plasmalemmal vesicles opened on the blood front of the endothelium (Figs. 9, 11 a, 11 b, 15 c, 21 c). They appear to penetrate more readily vesicles fully opened or provided with a neck, but they also gain access in smaller numbers to vesicles provided with a diaphragm (Figs. 11 b, 15 a, 15 c, 21 c). Past 4

[3] Tables II and III concern only glycogen particles. Corresponding data for dextrans were not collected because of difficulties introduced by particle heterogeneity, aggregation, and tendency to adsorb to endothelial surfaces.

min, tracer particles appear in increasing numbers in vesicles which seem to be isolated in the endothelial cytoplasm between the two fronts of the cell (Figs. 9, 10 a, 10 b, 15 a, 16), and past 6 min they mark many vesicles open on the tissue front of the endothelium (Figs. 10 c, 15 a, 16, 17). The labeling of plasmalemmal vesicles by dextrans, especially by D75, appears to be more pronounced than that achieved with glycogens (compare Figs. 10 b, 10 c, with Figs. 15 a and 16), but most of it seems to be due to particles smaller than the average size of the tracer. Hence, the difference could be explained by the higher degree of polydispersity of the dextrans; yet the affinity of the plasmalemmal membrane for dextrans deserves to be investigated, since often the concentration of the tracer appears higher in vesicles than in the lumen.

Table II gives the percentage of vesicles labeled by glycogens as a function of time and location within the depth of the endothelium. The figures show that a fraction of the vesicle population remains unlabeled at all times, that the frequency of the labeling increases with the time of exposure, and that at the early time points examined there is a gradient of decreasing labeling from the blood front to the tissue front of the endothelium. On each cell front, plasmalemmal vesicles are marked by the tracers irrespective of their position: there is no noticeable difference in labeling between vesicles located in the perikaryon (Figs. 11 a, 11 b) and vesicles in the attenuated periphery of the cell. Over the intervals considered, there is no or little evidence of accumulation of tracer particles within endothelial phagosomes or lysosomes (Fig. 15 a).

The intercellular junctions were found constantly free of probe molecules (Figs. 5, 10 a, 10 b, 12, 20). The same applies to the intercellular spaces except for occasional tracer particles present in their distal end (past the junction proper) usually in regions in which the edges of the apposed cells are provided with plasmalemmal vesicles.

SUBENDOTHELIAL SPACE AND BASEMENT MEMBRANE: At the time of penetration through the fenestrae, tracer particles transiently accumulate in the subendothelial space against the basement membrane and form small clusters opposite permeable fenestrae (Figs 5–8, 15 b, 20). There is a sharp drop in tracer concentration within the basement membrane proper, and a tendency of the particles to spread laterally in the subendothelial space so that in sections the clusters often appear as rows of particles (Figs. 5, 6 b, 6 c). These accumulations are more evident for glycogens than for dextrans and decay relatively rapidly so that by ~5 min they are no longer visible. Concentrations of tracers in the basement membrane are low at all time points examined; the membrane contains only rare glycogen particles and is marked by few recognizable dextran molecules of large size; the marking by small dextran particles is more frequent and occasionally rather pronounced (Figs. 2 b, 15 a, 16).

There is evidence of uptake of the tracers by the pericytes of the tunica media via plasma-

FIGURES 7 a–7 b Blood capillary 5 min after an i.v. injection of shellfish glycogen. Serial, nonconsecutive sections through a fenestrated part of the endothelium. They illustrate the formation of concentration gradients of tracer particles in the pericapillary spaces, opposite fenestrated parts of the endothelium (between arrows). Such gradients are more pronounced and lasting when formed, as in this case, in narrow interstitia. × 50,000.

FIGURE 8 Blood capillary 7 min after an i.v. injection of rabbit liver glycogen. The micrograph shows an attenuated part of the endothelium provided with three fenestrae (f_1–f_2) and a doubly diaphragmed channel (*ch*); f_2 appears impermeable, while f_1 and f_3 have allowed the passage of tracer particles retained at this time point by the basement membrane (*bm*). Note that the permeable fenestra f_2 appears to have a well defined diaphragm. × 81,000.

FIGURE 9 Blood capillary 4 min after an i.v. injection of shellfish glycogen. Unevenly attenuated part of the endothelium provided with fenestrae (f_1–f_3), a channel (*ch*), and plasmalemmal vesicles (v_1–v_4). Tracer particles mark two vesicles (v_3–v_4) and the channel. A particle has traversed the fenestra (f_1), and a few (*t*) have reached the pericapillary spaces. × 50,000.

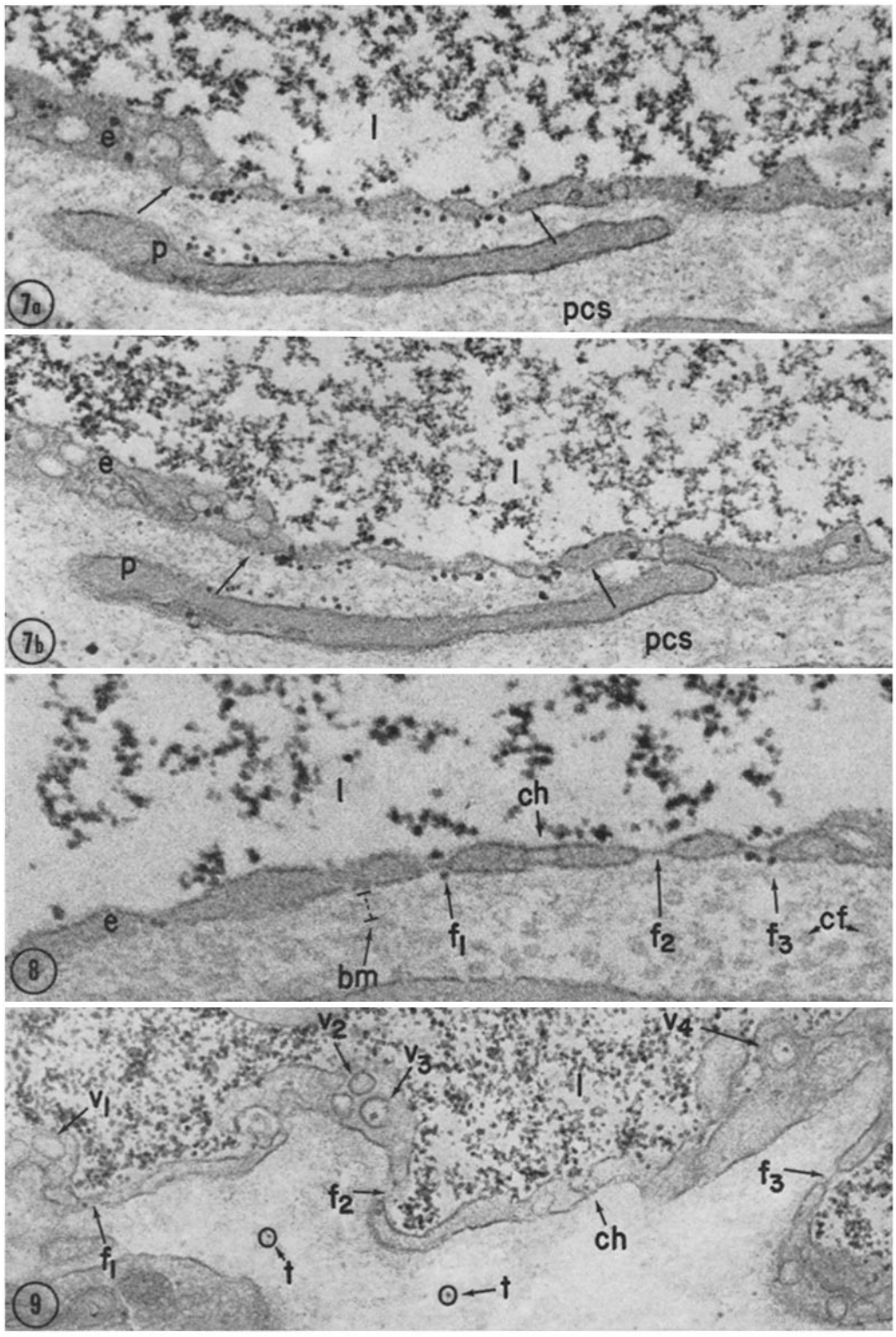
e
l
p
pcs
7a
e
l
p
pcs
7b
l
ch
e
bm
f1
f2
f3
cf
8
v2
v3
v4
v1
l
f2
f3
f1
ch
t
t
9

TABLE II

Tracer Particles in Endothelium and Pericapillary Spaces

Tracers	Time points	Fenestrae and channels: Marked/total	Fenestrae and channels: Particles/permeated fenestra	Fenestrae and channels: Particles in fenestrated parts of pericapillary space/fenestra	Vesicles: Marked/total: Luminal front	Vesicles: Marked/total: Inside	Vesicles: Marked/total: Tissue front	Vesicles: % Marked*	Vesicles: Particles in nonfenestrated parts of pericapillary space/vesicle
	min								
Shellfish	4	10/15	5.8	3.2	2/6	1/11	0/7	12.5	0.4
glycogen	5	3/11	3.6	8.3	3/9	4/12	5/11	37.5	3.4
Rabbit liver	6	9/13	1.7	1.2	1/5	0/10	0/11	3.8	0.4
glycogen	8	6/11	4.5	2.8	3/7	1/8	3/7	31.8	1.3
	11	5/11	1.2	4.3	2/7	3/6	5/8	47.6	3.1

For each time point, eighteen micrographs were used.

* In all positions.

For the definition of pericapillary spaces, see legend to Table III.

lemmal vesicles but no evidence of extensive accumulation in phagosomes.

ADVENTITIA AND PERICAPILLARY SPACES: There is considerable variation from capillary to capillary, even within the same region of the villus, about the time at which the tracer is first found in the pericapillary spaces, but in general probe particles begin to be detected in these spaces at about the same time or shortly after their emergence in the subendothelial space. Initially, they form concentration gradients with maxima centered on the fenestrated parts of the endothelium, and minima located opposite thicker, nonfenestrated segments (Fig. 5). These gradients have a short existence (Table III); past 5–8 min they can no longer be detected. Such concentration gradients persist for longer times and are more pronounced in cases in which the endothelial fenestrae open into a narrow interstitium, between the endothelium and pericytes, for instance (Figs. 7 a, 7 b). The data in Table III also show how low the efficiency is with which glycogen particles are transported across the capillary wall. By 6 min, the concentration of SG particles in the pericapillary spaces reaches only 7–8% of their concentration in the

FIGURE 10 a–10 c Blood capillaries 7 min after an i.v. injection of rabbit liver glycogen. The micrographs illustrate the presence of tracer particles in: (1) channels (ch_1), including channels provided with an intermediary diaphragm (ch_2) (the result of the recent fusion of two plasmalemmal vesicles); (2) plasmalemmal vesicles located within the endothelial cytoplasm (v_1–v_2), approaching (v_3) the tissue front of the endothelium or opened (v_4) on this front. The stoma of v_4 is provided with a diaphragm. The intercellular junctions (j_1 sectioned normally; j_2 sectioned in part obliquely) in Figs. 10 a and 10 b are not penetrated by the tracer. Note the difference in appearance between the exogenous glycogen used as a tracer and the endogenous glycogen (*ge*) present in the endothelial cytoplasm. Fig. 10 a, × 66,000; Fig. 10 b, × 78,000; Fig. 10 c, × 72,000.

FIGURES 11 a–11 b Blood capillaries 4 min after an i.v. injection of shellfish glycogen. Both figures demonstrate the presence of the tracer in plasmalemmal vesicles at the level of the perikaryon of endothelial cells. In Fig. 11 a, a vesicle (v_1) near the blood front of the endothelium is labeled by a multiplicity of tracer particles. In Fig. 11 b, two vesicles (v_2, v_3) along the same front are labeled by one or more tracer particles; v_2 appears to be fully open to the plasma; v_3 is provided with a stomatal diaphragm. Endogenous glycogen (*ge*) is present in clusters or as isolated particles. Fig. 11 a, × 76,000; Fig 11 b, × 80,000.

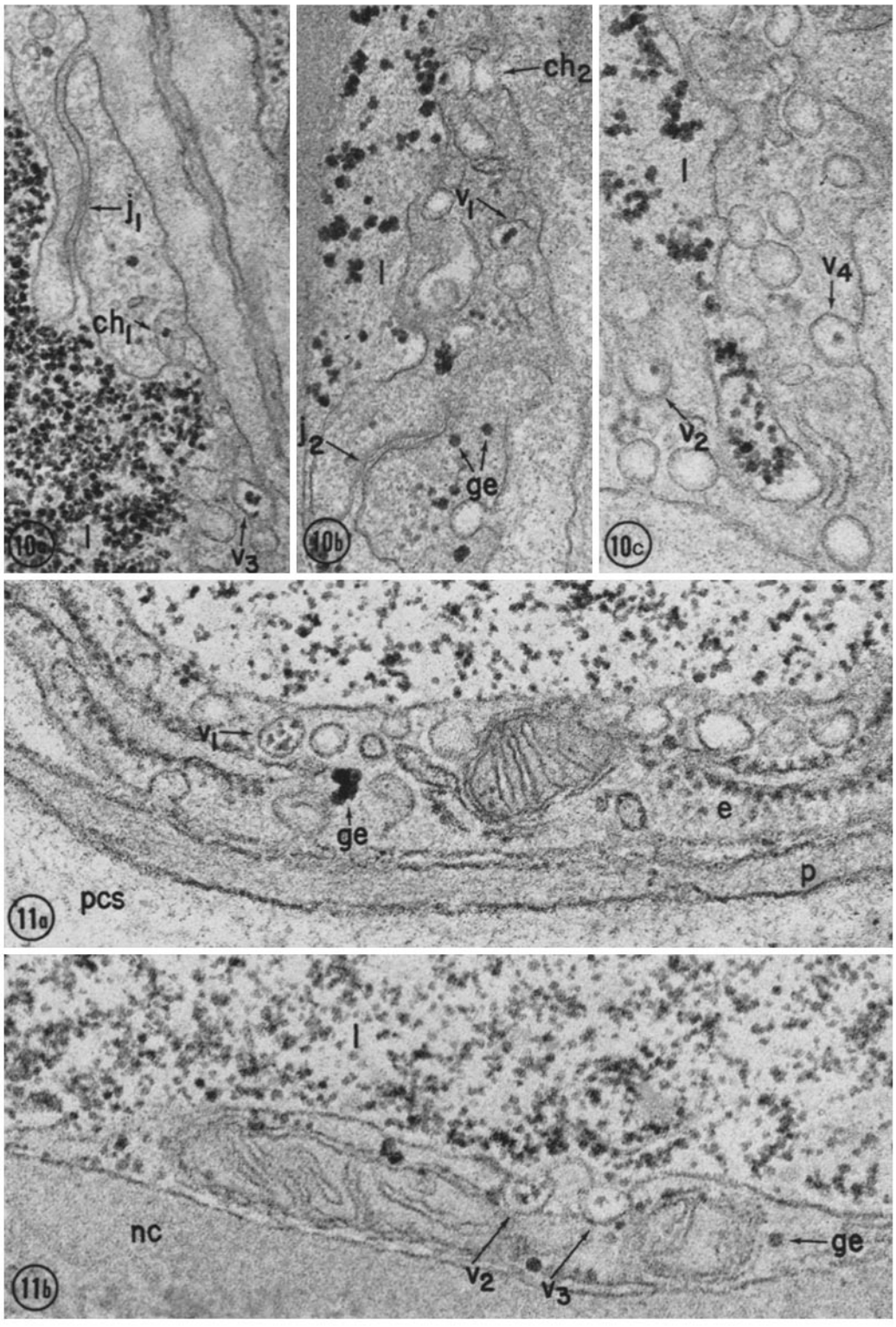
j_1
ch_1
l
v_3
10a
ch_2
v_1
l
j_2
ge
10b
l
v_4
v_2
10c
v_1
ge
e
p
pcs
11a
l
nc
v_2
v_3
ge
11b

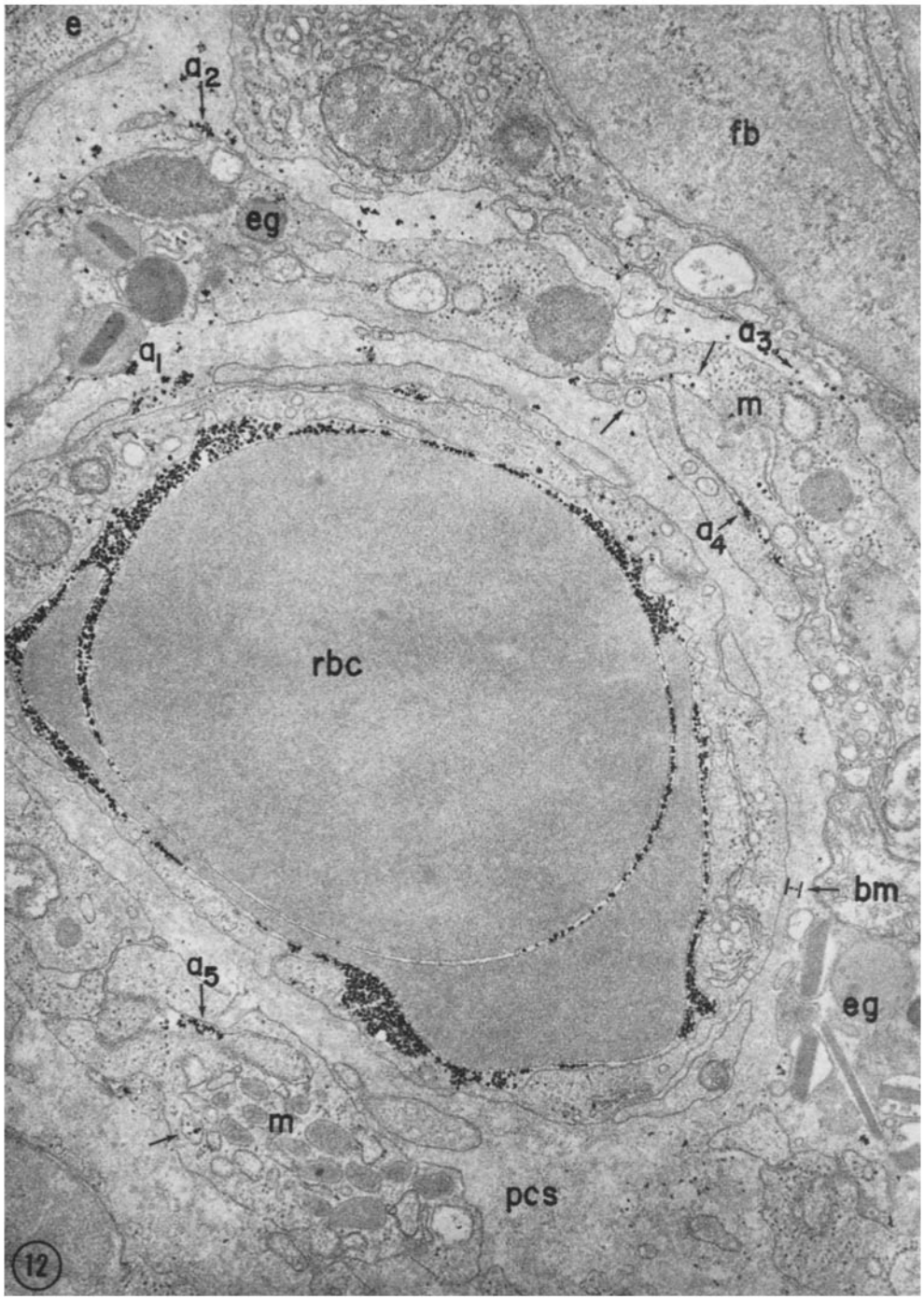

FIGURE 12 Blood capillary 8 min after an i.v. injection of rabbit liver glycogen. The micrograph illustrates the wide but uneven distribution of tracer particles in the pericapillary spaces at this time point. Glycogen particles appear to accumulate in recesses within the tunica media (a_1) and in narrow interstices between the cellular elements in the pericapillary spaces (a_2–a_5). The basement membrane (*bm*) and the relatively open interstitia in the pericapillary spaces (*pcs*) are nearly free of tracer. At this time point there is little evidence of endocytic activity (arrows) by macrophages and other cellular elements. × 22,000.

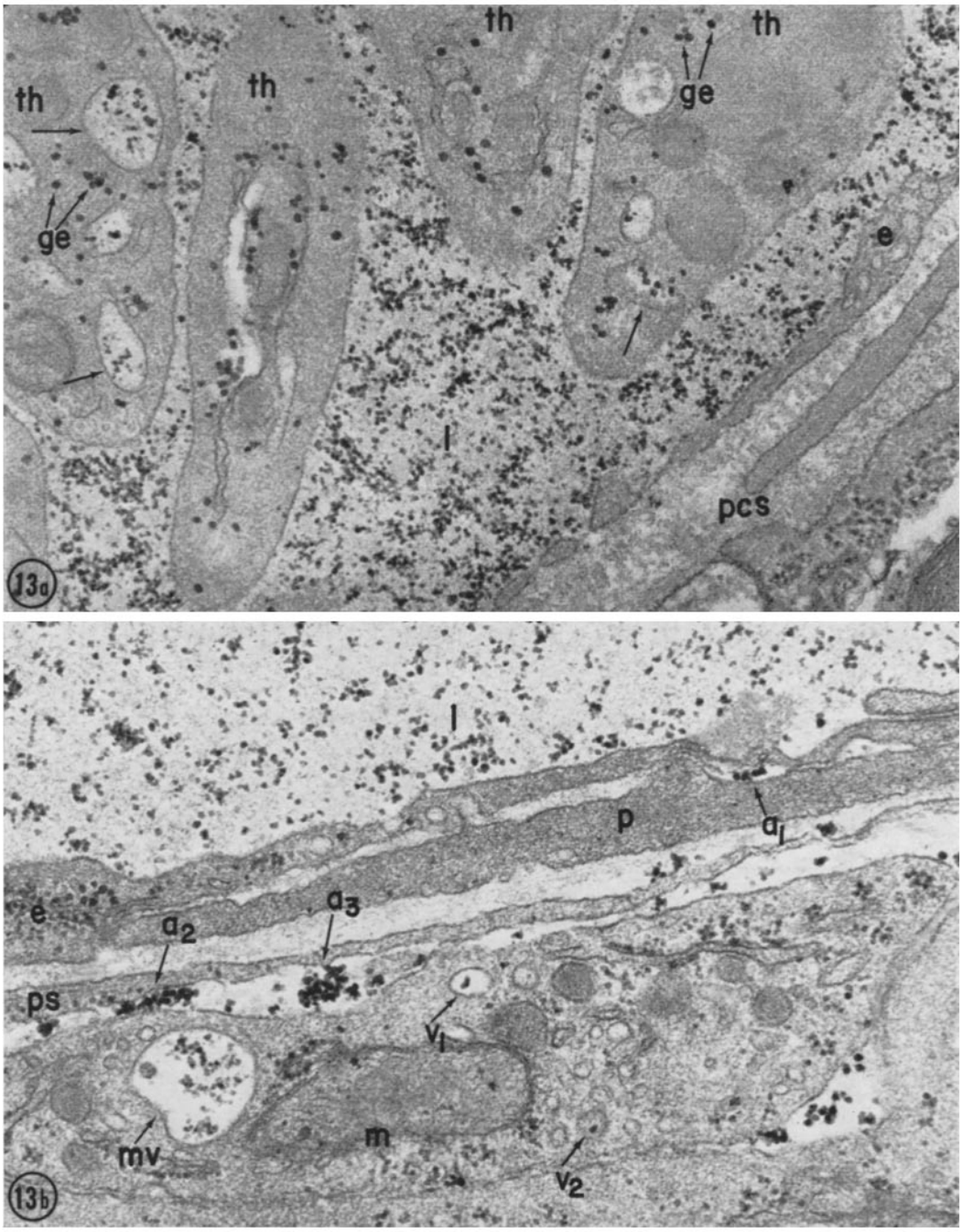

FIGURES 13 a–13 b Blood capillaries 4 min (Fig. 13 a) and 11 min (Fig. 13 b) after an i.v. injection of rabbit liver glycogen. Fig. 13 a shows the relatively active uptake of tracer particles by thrombocytes (*th*) in vacuoles of varied sizes (arrows). Note the difference in size and density between endogenous (*ge*) and exogenous glycogen particles. Fig. 13 b shows the accumulation of glycogen particles between the endothelium and a pericyte (a_1) and between the pseudopodium (*ps*) of an unidentified cell and a macrophage (a_2, a_3). Glycogen particles taken up by the macrophage appear in a multivesicular body (*mv*) and in a few vesicles of varied sizes (v_1, v_2). × 50,000.

plasma. For RLG particles the corresponding value is 6–7% by 11 min. Except for the immediate vicinity of the vessel, the distribution of the tracer in the pericapillary spaces appears to be uneven (Figs. 2 b, 12, 16), a feature that becomes more pronounced as the over-all concentration of tracer particles in these spaces increases with time. Over the short intervals, so far considered, there is little evidence of accumulation of tracers within the cellular elements of the adventitia, i.e. in macrophages (Figs. 12, 13 b), and fibroblasts.

In summary, the salient early events established are: *in the endothelium*, striking labeling of certain fenestrae by the probes used, and apparently random distribution of permeable fenestrae over the fenestrated parts of the endothelial tunic; *in the pericapillary spaces*, the early formation of transient gradients of probe particles, centered on the fenestrated sectors of the endothelium.

Late Events (from 16 Min to 24 Hr)

PLASMA: The concentration of glycogen particles in the circulating plasma decreases relatively rapidly: by 2 hr it is noticeably reduced, and by 4 hr few or no particles are left in the vascular lumina. By contrast, the concentration of dextrans decreases much more slowly so that 24 hr after the beginning of the experiment the plasma is still labeled (Fig. 18).

ENDOTHELIUM: Glycogen labeling of fenestrae and vesicles increases progressively over the first 1 or 2 hr so that a distinction between permeable and nonpermeable fenestrae is no longer possible. The labeling of the vesicles open on the tissue front of the endothelium becomes extensive, but by now the concentration of probe molecules in the pericapillary spaces is high enough to render uncertain the direction of the movement of the tracer. Past 4 hr the endothelium is free of glycogen particles. Dextran behavior in the endothelium is similar to that of glycogen, except that the tracer is still present in fenestrae and vesicles past 24 hr.

PERICAPILLARY SPACES: At about 16–30 min, the average concentration of particles in the pericapillary spaces approaches the concentration in the plasma but in detail it varies from one domain to another: few or no particles are seen within bundles of collagen fibrils and most of the probes are restricted to areas free of structured components. Moreover, glycogen particles often tend to form small aggregates, especially in the narrow intercellular interstitia of the pericapillary spaces (Figs. 12, 13 b). There is little accumulation of glycogen in macrophages at any time point and the pericapillary spaces become free of such tracers by ~4 hr, like the plasma. Dextran particles are still present in the pericapillary spaces past 24 hr, but there is little morphological evidence of dextran uptake by local macrophages.

Ferritin

The results obtained with ferritin are similar to those already described in the blood capillaries of the intestinal mucosa of the mouse (1).

FIGURE 14 Blood capillary 1.5 min after an i.v. injection of dextran 75. The dextran particles in the plasma are rather heterogeneous in size and shape (from filamentous to globular). The larger, more irregular particles in the right side of the lumen are probably the result of local aggregation (*ag*). At this time point, and in this field, no particles are found in transit through the endothelium and only occasional particles (*t*) are seen in the pericapillary spaces. × 55,000.

FIGURES 15 a–15 c Blood capillaries 3 min after an i.v. injection of dextran 75. At this time dextran particles are seen in transit through endothelial channels (*ch*) and in plasmalemmal vesicles. The latter are either open on the luminal front (v_1, v_2, v_4–v_8), enclosed within the cytoplasm (v_3, v_9), or open on the tissue front (v_{10}) of the endothelial cells. Note that some of the labeled vesicles (v_6, v_7, and v_{10}) have well defined stomatal diaphragms. Some particles have apparently traversed diaphragmed fenestrae (f_1, f_2) and appear located in the subendothelial space in between the fenestral diaphragms and the basement membrane (*bm*). Note that dextran particles tend to aggregate in some cases within plasmalemmal vesicles (v_1, v_4, v_5), or in the vicinity of the luminal membrane of the endothelium. At 3 min numerous dextran particles (*t*) are already found in the pericapillary spaces; note that most of them are in the range of the small to medium sized particles seen in the plasma. The negative images in Fig. 15 a represent transversely cut collagen fibrils (*cf*). The body marked *ly* in Fig. 15 a is a lysosome which seems to contain a few small-sized dextran particles. Fig. 15 a, × 50,000; Fig. 15 b, × 68,000; Fig. 15 c, × 72,000.

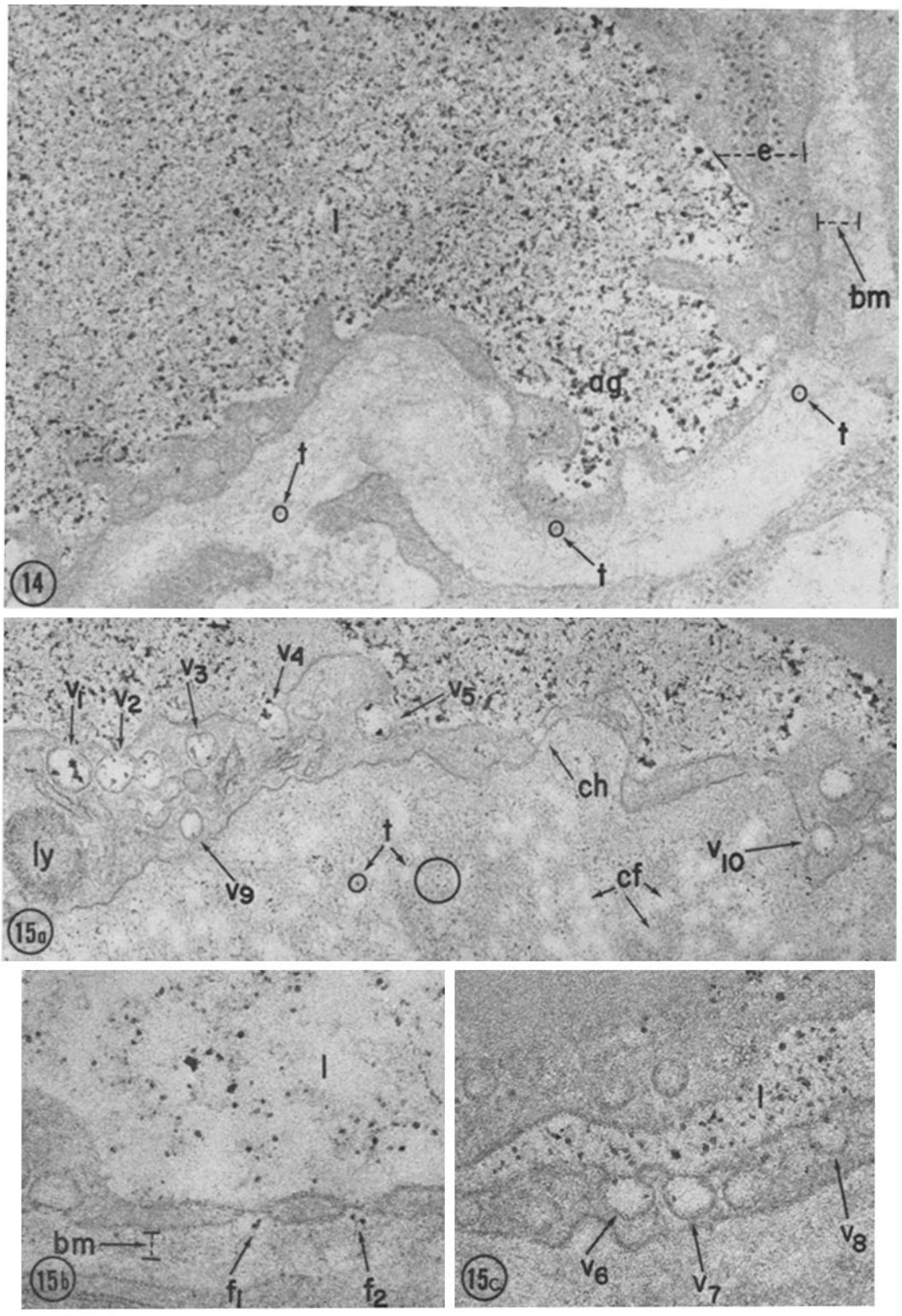
e
l
bm
dg
t
t
t
14
v1
v2
v3
v4
v5
ch
ly
t
v9
v10
cf
15a
l
bm
f1
f2
15b
l
v6
v7
v8
15c

TABLE III

Tracer Particles Concentration in the Capillary Lumina and Pericapillary Spaces
(Number of particles: μ^2 section)*

Tracer	Time points	Capillary lumen	Pericapillary spaces‡				
			Opposite fenestrated endothelium (A)		Opposite nonfenestrated endothelium (B)		
			Particles · μ^2	% of particle concentration in lumen	Particles : μ^2	% of particle concentration in lumen	Ratio A:B
	min						
Shellfish glycogen	4	2542 ± 149	60 ± 11	2.3	16 ± 5	0.6	3.7
	6	1969 ± 188	138 ± 21	7.0	154 ± 22	7.8	0.8
Rabbit liver glycogen	6	2244 ± 206	32 ± 5	1.4	4 ± 1	0.1	8.0
	8	1681 ± 99	74 ± 10	4.4	38 ± 9	2.2	1.9
	11	1396 ± 141	89 ± 19	6.3	99 ± 17	7.0	0.9

* For each time point, eighteen micrographs were used: the aggregate areas counted for each interval ranged from 17 to 22 μ^2 for the lumen, from 5.0 to 6.2 μ^2 for the A areas, and from 3.3 to 5.5 μ^2 for the B areas of the pericapillary spaces.

‡ Defined as the space limited on the inner side by the capillary basal membrane and on the outer side by the epithelial basement membrane, cellular elements of the lamina propria and, in between such elements, by arbitrary lines extending the boundaries mentioned. Particles in the subendothelial spaces or basement membrane are not included among the particles counted in the pericapillary spaces. These spaces, which range in depth from ~3000 A to 4500 A, have been subdivided for convenience in two parts facing the fenestrated (A) and nonfenestrated (B) regions of the endothelium, respectively.

DISCUSSION

We have used a series of five tracers ranging in molecular diameter from 100 to 300 A to explore the pathway followed by macromolecules across the blood capillaries of the intestinal mucosa in the adult rat. One of these tracers is a protein, ferritin, already used in a similar study in the mouse (1), the others are polysaccharides, namely glycogens and dextrans recently introduced as molecular probes for work on structural aspects of capillary permeability (6). Our previous results have established that polysaccharide particles are well tolerated, easily detectable tracers; the new results show that the glycogens remain in circulation for 3–4 hr, whereas the dextrans are still found in the plasma after 24 hr; they also show that the intestinal mucosa is not affected by long exposure to circulating polysaccharide tracers.

Since the capillary wall has a stratified structure (23, 24, 25) and the pathways appear to be different from tunic to tunic, they will be considered separately in the endothelium (inner tunic) and in the basement membrane (middle tunic).

Endothelium

Our results show that all particles tested follow the same pathways which can be divided into established and probable.

The fenestrae and channels are recognized as well established pathways on account of (*a*) the presence of probe particles within their lumina, (*b*) the appearance of transient clusters of particles in the subendothelial space opposite certain fenestrae and channels, and (*c*) the generation of transient concentration gradients of tracers in the pericapillary spaces with maxima centered on the fenestrated parts of the endothelium (Table III).

Permeable fenestrae appear to be randomly distributed in the total fenestral population and their proportion therein varies from 20 to 70% from one site to another along the inner tunic. Some of the unmarked fenestrae are undoubtedly permeable; they remain unlabeled on account of the random distribution and relatively low concentration of the tracers; some of them may be truly inpermeable but, with the available evi-

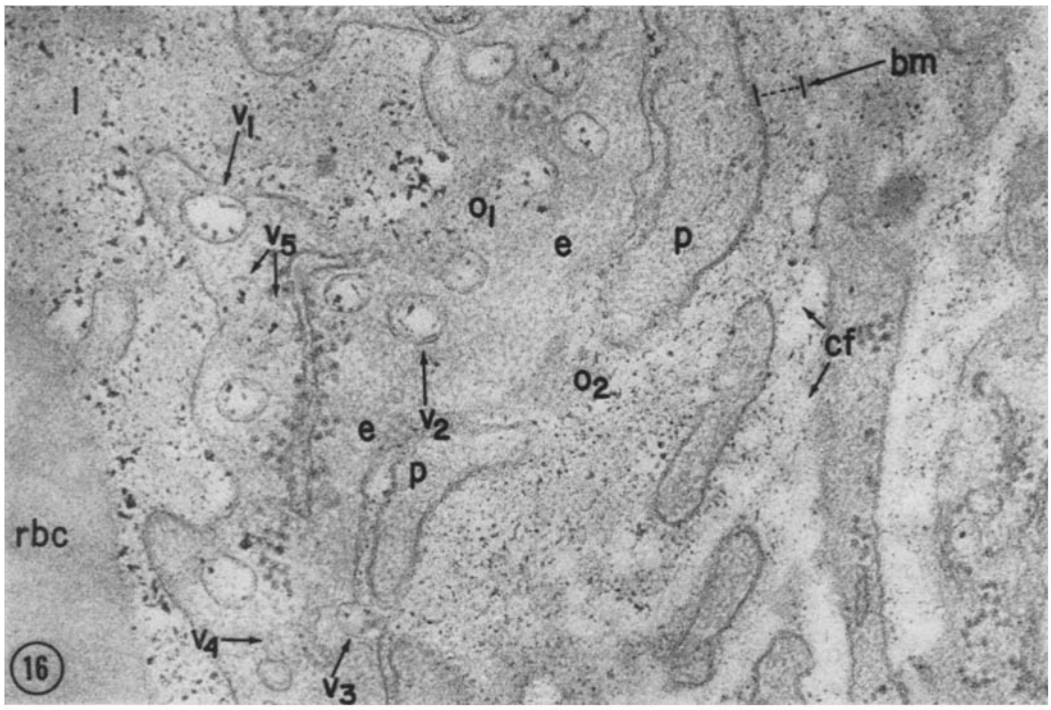

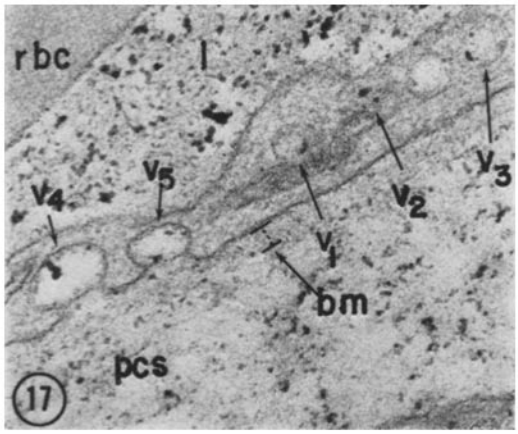

FIGURE 16 Blood capillary 8 min after an i.v. injection of dextran 75. At this time point practically all the plasmalemmal vesicles of the endothelium—including those half included (v_4, v_5) in the thickness of the section—are labeled by dextran particles irrespective of their adluminal (v_1), intracytoplasmic (v_2), or abluminal (v_3), location within the endothelium. Particles dot the areas where the endothelium is obliquely cut and either part of the lumen (o_1) or part of the subendothelial space (o_2) is included in the sections. The concentration of particles in the interstitia between endothelium and pericytes, in the basement membrane (*bm*) and in the pericapillary spaces has increased and particle size ranges on the two sides of the endothelium are nearly equal (except for luminal aggregates). × 70,000.

FIGURE 17 Blood capillary 11 min after an i.v. injection of dextran 75. All plasmalemmal vesicles in this field are labeled, including those half included in the thickness of the section (v_1–v_3) and those open (v_4, v_5) on the tissue front of the endothelium. The latter are provided with stomatal diaphragms. × 81,000.

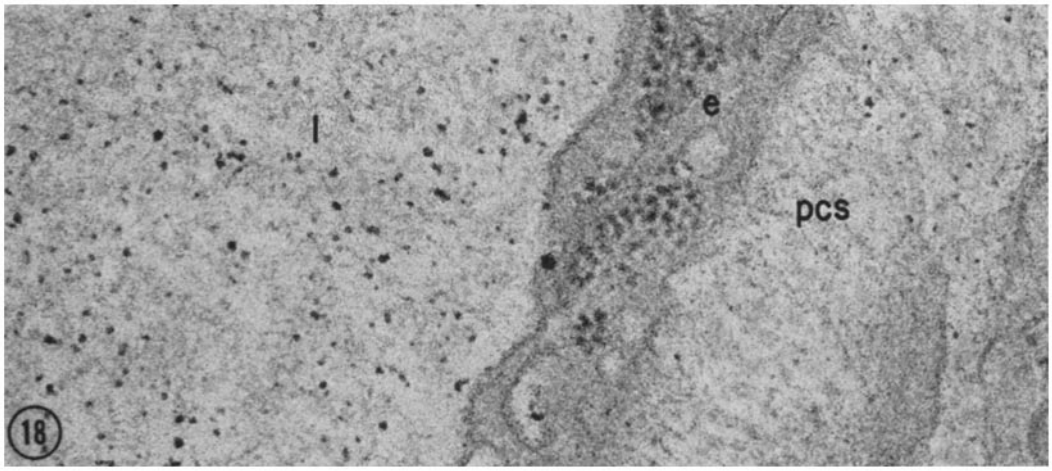

FIGURE 18 Blood capillary 24 hr after an i.v. injection of dextran 75. Note that a relatively high concentration of particles is still present in the plasma and in the pericapillary spaces (*pcs*); note also that the particles in the pericapillary spaces are on the average smaller than those in the lumen. × 90,000.

dence, we cannot ascertain whether the fenestrae and channels belong to two distinct types, i.e. permeable and impermeable, or whether the two forms are interconvertible.

No correlation can be established between permeability and absence of diaphragms within the fenestral population. Such a correlation was considered in (1), but in the present investigation most of the fenestrae, including those evidently permeable, appeared to be provided with diaphragms. It is noteworthy that large dextran particles appear to unravel when passing through the fenestrae. We should stress again, however, that the morphological evidence at hand (1, 26–31) cannot indicate how continuous or discontinuous the fenestral diaphragms are.

The probable pathway is represented by the plasmalemmal vesicles. In their case, we do not have the type of conclusive evidence supplied by concentration gradients in the subendothelial and pericapillary spaces we found associated with fenestrae and channels, but we assume that they participate in tracer transport for the following reasons: (*a*) they are extensively labeled by the tracers, initially on the blood front and later on in the endothelial cytoplasm and on the tissue front; (*b*) there is no accumulation of the tracers in endothelial phagosomes or lysosomes commensurate with the extent of vesicular uptake; (*c*) in muscle capillaries (i.e., in vessels with a continuous, nonfenestrated endothelium), plasmalemmal vesicles have been shown to function in macromolecular transport (32). Our assumption is strengthened by morphological findings which suggest that vesicles, fusing vesicles, channels, and fenestrae are successive aspects of a common dynamic system (33). The lack of pericapillary gradients centered on vesicles could be explained by the slowness of vesicular transport and by the rapid diffusion of particles escaping through fenestrae and channels. The data in Table II (compare column 5 to column 10) suggest that at the earliest time points transport by vesicles is at best three to eight times slower than exit through fenestrae.

Basement Membrane

There are no structurally recognizable pathways across the basement membrane; the findings suggest that this tunic is generally and extensively porous. An observation that deserves comment is the transient accumulation of tracer particles in the subendothelial space opposite certain permeable fenestrae. It indicates that the endothelium can be easily cleaved away from the basement membrane, at least over limited domains, and it raises a number of interesting questions. If the accumulation is physiological, then the pathways across the two tunics are not necessarily in phase and a particle transported across the endothelium may diffuse in the subendothelial

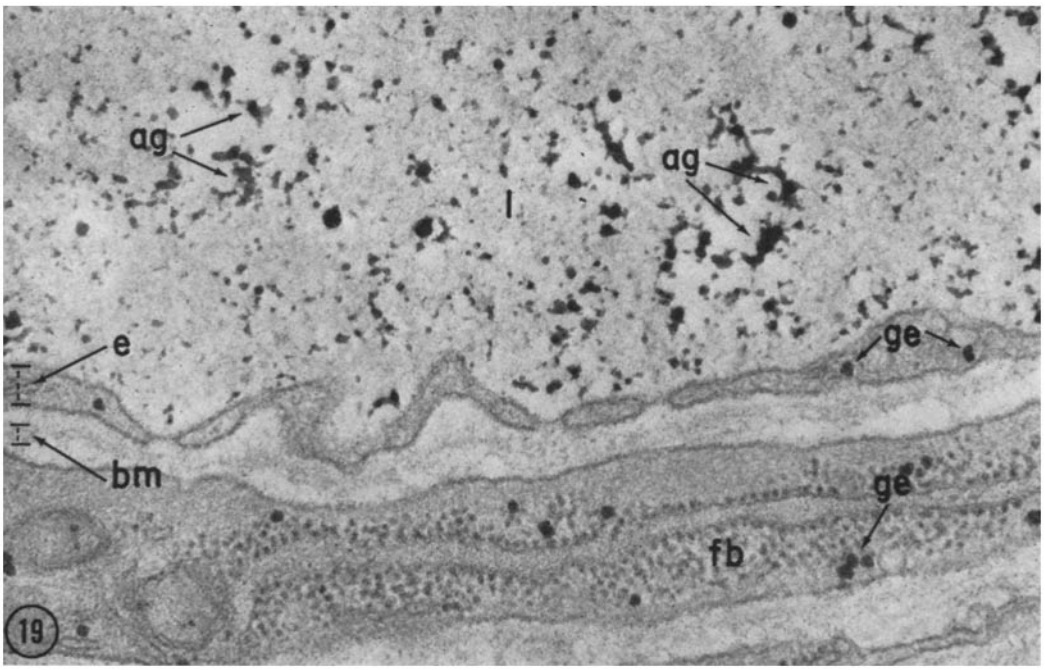

FIGURE 19 Blood capillary 2 min after an i.v. injection of dextran 250. The tracer particles in the plasma appear polymorphous and heterodispersed and tend to form local aggregates (*ag*) of large size. At this time point and in this field, there are no particles in transit through the fenestrated endothelium and no particles in the pericapillary spaces. Endogenous glycogen in the endothelium (*e*) and an adjacent fibroblast (*fb*) is marked *ge*. × 62,000.

space until it encounters a passage of adequate dimensions across the basement membrane. This point has already been discussed in (34) in relation to larger particles. The transient character of these accumulations and the fact that the subendothelial spaces usually appear collapsed suggest that we may be dealing with a temporary disturbance in the rate of transport across the two tunics of the wall. A temporary stretching of the endothelial fenestrae without commensurate stretching of the porosity of the basement membrane could produce such accumulations. We intend to investigate this aspect in further detail.

Correlations with the Pore Theory

Physiological data on the permeability of intestinal capillaries to large molecules are currently rationalized by assuming the existence of a system of large water-filled channels or pores across the capillary wall (2–5, 35). There is wide agreement as to the existence of such "leaks," but no consensus as to their size and frequency. Mayerson et al. (3) estimate the diameter of the large pores at >280 A,–their aggregate area at ∽21.6% of the total (small + large) pore surface,–the diameter of the small pores at ∽220 A,–and incidentally consider the possibility that the function of the large pores is carried out by plasmalemmal vesicles. From Grotte's data (2) which refer primarily to other capillary beds, some of them similar to that of the intestine, we can estimate the fractional area of the large pores as larger than 1% but smaller than 10% of the total pore surface. Grotte (2) and Landis and Pappenheimer (4) calculate the diameter of the large pore at 400–700 A and that of the small pores at ∽90 A.

Our results can be used to identify the structural equivalents of the large pore system in the capillaries of the intestinal mucosa of the rat, and to resolve in part the lack of agreement mentioned above.

Our tracers range in diameter from 100 to 300 A and hence span a reasonably large fraction of the assumed diameter of the large pores. Since all

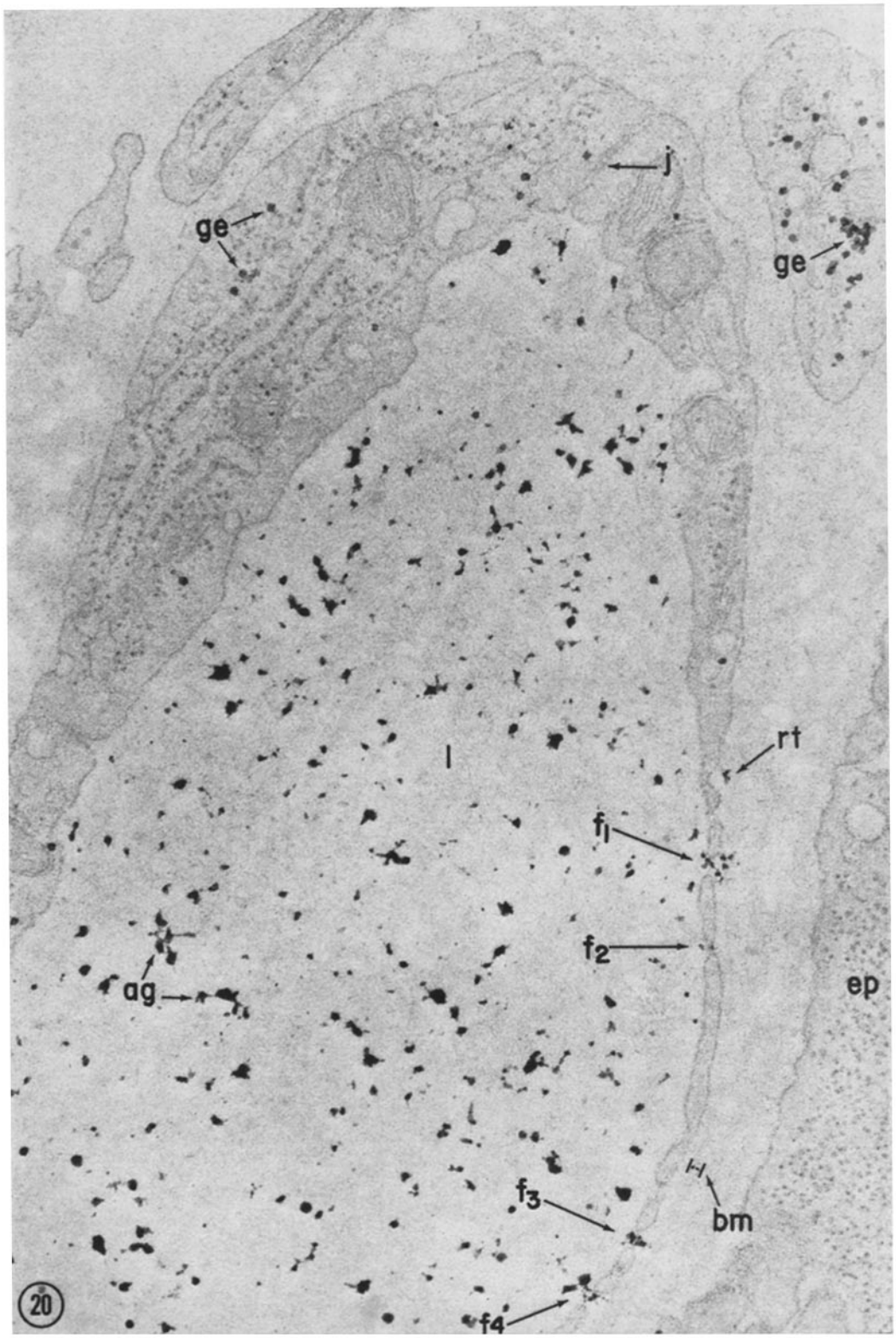

FIGURE 20 Blood capillary 4 min after an i.v. injection of dextran 250. As in Fig. 19, the particles in the lumen are polydispersed, polymorphic, and tend to form local aggregates (*ag*). The fenestrated part of the endothelium is directed towards the intestinal epithelium (*ep*). Tracer molecules are in transit through some (f_1–f_4) but not all of the fenestrae in the area, and most of the escaping particles seem to be retained (f_1–f_4 and *rt*) by the basement membrane (*bm*). Two impermeable fenestrae can be seen between f_2 and f_3. Note that the molecules or aggregates in transit through the fenestrae seem to unravel as they go through (at f_1 and f_4). Note also that no particles escaped through the intercellular junction (*j*) or through the nonfenestrated part of the endothelium in the upper left part of the capillary profile. × 32,000.

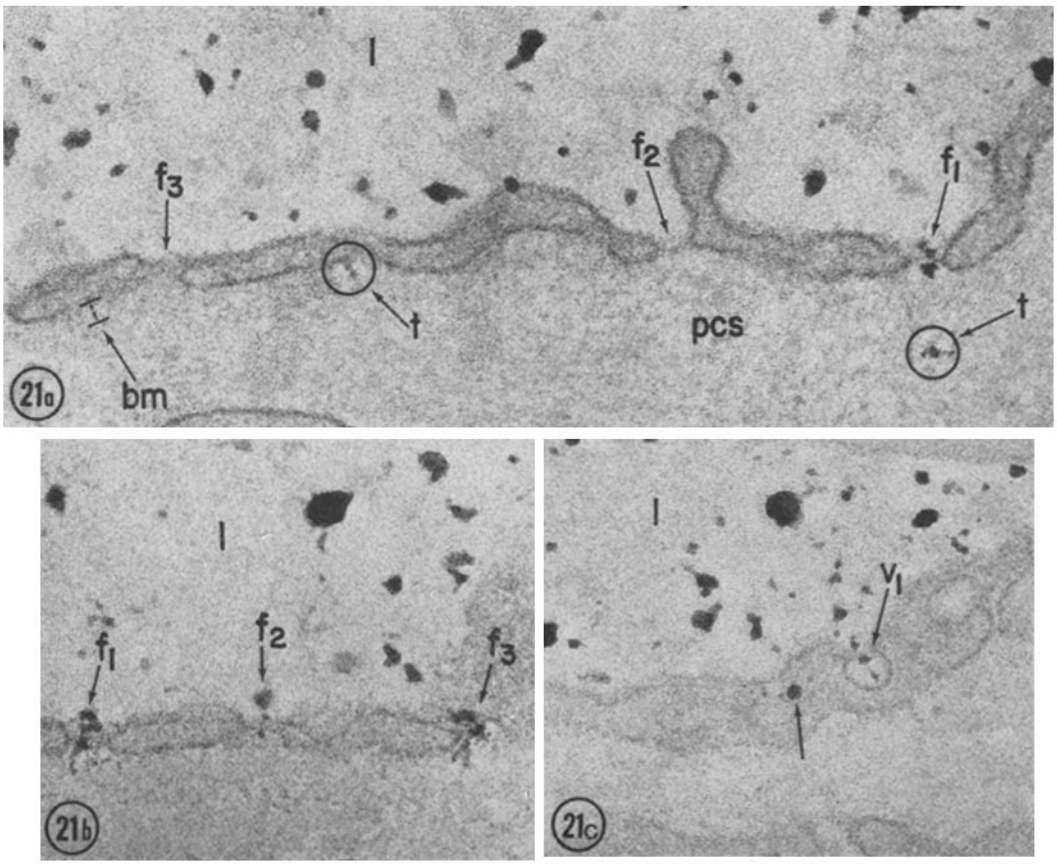

FIGURES 21 a–21 c Blood capillaries 4 min after an i.v. injection of dextran 250. For the condition of the tracer in the lumen, see the legend to Figs. 19 and 20. Fig. 21 a shows that the tracer was moving at the time of fixation through some (f_1), but not all of the fenestrae (f_2, f_3) of the endothelium. Few particles (t) are already present in the basement membrene (bm) and the pericapillary spaces. Fig. 21 b illustrates dextran particles (or aggregates) in transit through three adjacent fenestrae (f_1–f_3). The particles in f_1 and f_2 seem to unravel as they pass. Fig. 21 c shows tracer particles in a plasmalemmal vesicles (v_1) opened on the blood front of the endothelium. Fig. 21 a, × 78,000; Fig. 21 b, × 82,000; Fig. 21 c, × 62,000.

these tracers leave the plasma definitely through fenestrae and channels and probably through vesicles, all these devices are recognized as structural equivalents of the large pore system in the endothelial tunic. The morphological findings are in general agreement with the physiological data, since they reveal that these graded tracers follow a common pathway which, in the case of the fenestrae and channels, comes very close to the physiological postulate of a water-filled channel. In these structures the continuity of the channel across the endothelium is interrupted only by one or two diaphragms, i.e. by structures which appear to be highly permeable to water and water-soluble molecules.

There is partial agreement as to the dimensions, although for complete agreement particles in the range of 400–700 A should be tested in further experiments.[4] We should point out, however,

[4] Moreover, since ferritin (diameter = 110 A) leaves the plasma through a comparable fraction of the total fenestral population as the other tracers, we can conclude that in the rat the small pores are smaller than 110 A as estimated from Grotte's data (2) rather than 220 A wide as postulated by Mayerson (3). This conclusion supports the view expressed by Clementi and Palade (1) who, in work on the capillaries of the intestinal mucosa of the mouse, used ferritin as a tracer, assumed that it escapes exclusively through large pores, and tentatively identified ferritin-permeable fenestrae as the structural equivalent of the large pore system.

that according to the pore theory the large pores are considered to be all of equal dimensions, whereas the existence of fenestral diaphragms introduces the possibility of restrictions within the pathways and of heterogeneity within the total fenestral population.

There is no agreement as to frequency. Calculations based on Grotte's (2) and Mayerson's data (3) give, for the total large pore area, estimates of the order of 0.05% of the endothelial surface, whereas the estimate for the aggregate area of the fenestrae is ∽10% of the same surface. This large discrepancy can be explained only partially by the fact that not all the fenestrae appear to behave like large pores, and by the fact that there is retention of tracers in the cellular elements of the adventitia.

The discrepancy remains an open question for which there is no satisfactory answer at present. It is probable that the concentration of tracer particles in the vascular lymph is considerably lower than in the interstitial fluid. Moreover, it is possible that the diaphragms are labile structures with rapidly changing porosity. They may function as large pores for intervals of the order of seconds or fractions of seconds, while the micrographs may record their behavior over considerably longer periods so that the number of fenestrae acting as large pores may appear greatly increased.

There is no recognizable structure in the basement membrane that can be identified as the equivalent of a large pore in the middle tunic. The impression is that the size limiting channels are located in the endothelium and that large pores are relatively frequent in the basement membrane since in general there is no lasting retention of particles by this layer. Yet there is no explanation at present for the fact that discontinuities of the expected size are not seen in the middle tunic.

In the adventitia and pericapillary spaces, the distribution of tracers is quite heterogeneous: the large particles appear to be restricted to relatively structure-free channels left among cells and fibrillar masses, while the small particles penetrate practically all fine interstitia within the basement membrane and within fibrillar bundles. The appearance of these spaces is reminiscent of a heterogeneous gel system with accessible and restricted domains (36, 37). This type of distribution most probably affects plasma-lymph exchanges, especially in their initial phase. Hence, this kind of gel filtration is another correction to be considered, in addition to general retention and phagocytosis within the tissue, in interpreting lymph: plasma concentration gradients, especially in studies dealing with rates of appearance of different tracers in the lymph.

The final question to be discussed concerns the location of the large pores along the vascular bed of the intestinal mucosa. Permeable fenestrae and channels and labeled vesicles have been encountered along all the capillaries of the villi and, for the moment at least, there is no firm indication that the frequency increases in certain parts of the villi or in certain segments of the villus vasculature. Hence, it can be tentatively concluded that the large pores are about evenly distributed in this vascular bed. We recognize, however, that in our material and in our conditions we cannot identify the arteriolar and venular ends of the capillary bed. In other situations, in which these ends can be easily recognized, i.e. mammalian muscle (38, 39), frog skin (40), and frog mesentery (41, 42), there is evidence indicating that slowly diffusible dyes, presumably large molecules, preferentially leave the vasculature through the venous end of capillaries and collecting venules, presumably on account of a high concentration of "leaks" at that level. It would be interesting to find out whether large pore equivalents of the type discussed in this paper are the structural basis of these rather massive leaks, and whether such equivalents are more concentrated on the venous side of the vasculature. This problem should be investigated on specimens geometrically more favorable than the vascular bed of intestinal villi.

We gratefully acknowledge the excellent technical assistance of Miss Jill Sapinsley, Mrs. Jane Deutsch-Musser, Miss Paula Sonnino, Mrs. Elizabeth Szabo, and Mr. Roland Blischke. We also thank David J. Castle for help with the statistics.

This work was supported by Public Health Service Grant HE 05648.

Received for publication 21 October 1971, and in revised form 4 January 1972.

REFERENCES

1. Clementi, F., and G. E. Palade. 1969. Intestinal capillaries. I. Permeability to peroxidase and ferritin. *J. Cell Biol.* 41:33.

2. GROTTE, G. 1956. Passage of dextran molecules across the blood-lymph barrier. *Acta Chir. Scand.* **211**(*Suppl.*):1.
3. MAYERSON, H. S., C. G. WOLFRAM, H. H. SHIRLEY, JR., and K. WASSERMAN. 1960. Regional differences in capillary permeability. *Amer. J. Physiol.* **198**:155.
4. LANDIS, E. M., and J. R. PAPPENHEIMER. 1963. Exchange of substance through the capillary walls. *In* Handbook of Physiology. W. F. Hamilton and P. Dow, editors. American Physiology Society, Washington, D. C. **II** (2).
5. RENKIN, E. M. 1964. Transport of large molecules across capillary walls. *Physiologist.* **7**:13.
6. SIMIONESCU, N., and G. E. PALADE. 1971. Dextrans and glycogens as particulate tracers for studying capillary permeability. *J. Cell Biol.* **50**:616.
7. GOTH, A., and M. KNOOHUIZEN. 1966. Genetically conditioned dextran cofactor in the rat. *Fed. Proc.* **25**:692.
8. ANDREW, W., and N. V. ANDREW. 1957. An age involution in the small intestine of the mouse. With a description of the fundamental process of lympho-epithelial metamorphosis in intestinal mucosa. *J. Gerontol.* **12**:136.
9. DURANT, R. R. 1927. Blood pressure in the rat. *Amer. J. Physiol.* **81**:679.
10. WANG, L. 1959. Plasma volume, cell volume, total blood volume and F cells factor in the normal and splenectomized Sherman rat. *Amer. J. Physiol.* **196**:188.
11. WOODBURY, R. A., and W. F. HAMILTON. 1937. Blood pressure studies in small animals. *Amer. J. Physiol.* **119**:663.
12. FERNANDEZ, L. A., O. RETTORI, and R. H. MEJIA. 1966. Correlation between body fluid volumes and body weight in the rat. *Amer. J. Physiol.* **210**:877.
13. WASSERMAN, K., and H. S. MAYERSON. 1954. Relative importance of dextran molecular size in plasma volume expansion. *Amer. J. Physiol.* **176**:104.
14. SEMPLE, R. E. 1954. Effect of small infusions of various dextran solutions on normal animals. *Amer. J. Physiol.* **176**:113.
15. KARNOVSKY, M. J. 1965. A formaldehyde-glutaraldehyde fixative of high osmolarity for use in electron microscopy. *J. Cell Biol.* **27**:137 A (Abstr.)
16. FARQUHAR, M. F., and G. E. PALADE. 1963. Junctional complexes in various epithelia. *J. Cell Biol.* **17**:375.
17. VYE, M. V., and D. A. FISHMAN. 1970. The morphological alteration of particulate glycogen by *en bloc* staining with uranyl acetate. *J. Ultrastruct. Res.* **33**:278.
18. MUMAW, V. R. and B. L. MUNGER. 1971. Uranyl acetate-oxalate an *en bloc* stain as well as a fixative for lipids associated with mitochondria. *Anat. Rec.* **169**:383 (Abstract).
19. LUFT, J. H. 1961. Improvements in epoxy embedding methods. *J. Biophys. Biochem. Cytol.* **9**:409.
20. ROCKWELL, A. F., P. NORTON, J. B. CAULFIELD, and S. I. ROTH. 1966. A silicone rubber mold for embedding tissue in epoxy resins. *Sci. Tools.* **13**:9.
21. VENABLE, J., and R. COGGESHALL. 1965. A simple lead citrate stain for use in electron microscopy. *J. Cell Biol.* **25**:407.
22. FRASCA, J. M., and V. R. PARKS. 1965. A routine technique for double-staining ultrathin sections using uranyl and lead salts. *J. Cell Biol.* **25**:157.
23. BENNETT, H. S., J. H. LUFT, and J. C. HAMPTON. 1959. Morphological classification of vertebrate blood capillaries. *Amer. J. Physiol.* **196**: 381.
24. BRUNS, R. R., and G. E. PALADE. 1968. Studies on blood capillaries. I. General organization of muscle capillaries. *J. Cell Biol.* **37**:244.
25. LUFT, J. H. 1966. Fine structure of capillary and endocapillary layer as revealed by ruthenium red. *Fed. Proc.* **25**:1773.
26. RHODIN, J. A. G. 1962. The diaphragm of capillary endothelial fenestrations. *J. Ultrastruct. Res.* **6**:171.
27. LUFT, J. H. 1964. Fine structure of the diaphragm across capillary "pores" in mouse intestine. *Anat. Rec.* **148**:307.
28. FRIEDERICI, H. H. R. 1968. The tridimensional ultrastructure of fenestrated capillaries. *J. Ultrastruct. Res.* **23**:444.
29. FRIEDERICI, H. H. R. 1969. On the diaphragm across fenestrae of capillary endothelium. *J. Ultrastruct. Res.* **27**:373.
30. MAUL, G. G. 1971. Structure and formation of pores in fenestrated capillaries. *J. Ultrastruct. Res.* **36**:768.
31. CASLEY-SMITH, J. R. 1970. Endothelial fenestrae: their occurrence and permeabilities, and their probable physiological roles. *Septième Congr. Int. Microsc. Electron. Grenoble.* 49.
32. BRUNS, R. R., and G. E. PALADE. 1968. Studies on blood capillaries. II. Transport of ferritin molecules across the wall of muscle capillaries. *J. Cell Biol.* **37**:213.
33. PALADE, G. E., and R. R. BRUNS. 1968. Structural modulations of plasmalemmal vesicles. *J. Cell Biol.* **37**:633.
34. CLEMENTI, F., and G. E. PALADE. 1969. Intestinal capillaries. II. Structural effects of EDTA and histamine. *J. Cell Biol.* **42**:706.

35. RENKIN, E. M., and D. G. GARLICK. 1970. Transcapillary exchange of large molecules between plasma and lymph. *In* Capillary Permeability. Alfred Benzon Symposium II. Ch. Crone and N. A. Lassen, editors. Academic Press Inc., New York. 553.
36. LAURENT, T. C. 1963. The interaction between polysaccharides and other macromolecules. 5. The solubility of proteins in the presence of dextran. *Biochem. J.* **86:**253.
37. LAURENT, T. C. 1970. The structure and function of the intercellular polysaccharides in connective tissue. *In* Capillary Permeability. Alfred Benzon Symposium II. Ch. Crone and N. A. Lassen, editors. Academic Press Inc., New York. 261.
38. ROUS, P., H. P. GILDING, and F. Smith. 1930. The gradient of vascular permeability. *J. Exp. Med.* **51:**807.
39. SMITH, F., and P. ROUS. 1931. The gradient of vascular permeability. II. The conditions in frog and chicken muscle, and in the mammalian diaphragm. *J. Exp. Med.* **53:**195.
40. ROUS, P., and F. SMITH. 1931. The gradient of vascular permeability. III. The gradient along the capillaries and venules of frog skin. *J. Exp. Med.* **53:**219.
41. LANDIS, E. M. 1926. The capillary pressure in frog mesentery as determined by microinjection. *Amer. J. Physiol.* **75:**548.
42. LEVICK, J. R., and C. C. MICHEL. 1969. The passage of T_{1824}-albumin out of individually perfused capillaries of the frog mesentery. *J. Physiol. (London).* **202:**114.